

Review of monolithic and matrix composite ceramic sandwich structures for integrated thermal protection in hypersonic vehicles

Jacob Bilsborough , Hayley Neilsen-Burke, Mehdi Khatamifar, Elsa Antunes ^{*}

College of Science and Engineering, James Cook University, Townsville, 4814, Australia

ARTICLE INFO

Handling Editor: Dr Uday Vaidya

Keywords:

Sandwich structure
Hypersonic vehicles
Monolithic ceramic
Ceramic matrix composites
Thermal protection system
Additive manufacturing
Periodic lattice structures

ABSTRACT

The success of modern hypersonic aircraft hinges on the development of insulative aerostructures capable of withstanding sustained aerodynamic heating at speeds greater than Mach 5. Sandwich structures with porous lattice-cores have become a promising area of research towards the development of lightweight, load bearing panels that offer enhanced insulative performance. The use of ceramics in structural applications has traditionally been limited due to their brittle fracture behaviour, poor impact resistance and limited manufacturability. However, advancements in material science have improved the versatility of modern ceramics and their unparalleled thermal properties cannot be ignored for the design of ultra-high temperature aerospace structures. This literature review investigates the use of ceramic sandwich structures as integrated Thermal Protection Systems (TPSs) of emerging hypersonic aircraft, including current materials and manufacturing trends, the performance of distinct core designs, and the current state-of-the-art integration of advanced thermal management methods. Current challenges associated with the design, development, and progress of ceramic sandwich structures in the context of hypersonic aerospace applications are discussed and future avenues of research are proposed.

1. Introduction

Airbreathing hypersonic systems are an emerging class of ultra-high-speed aircraft capable of sustained flight at speeds greater than Mach 5, or five times the speed of sound. These vehicles are predicated on the use of advanced supersonic combustion ramjet (scramjet) engines that have the capacity to operate within a Mach number range of 4–12 using carbon neutral fuel sources [1,2]. Hypersonic aircraft are designed to maximise the functional potential of scramjet engines by providing a reusable and efficient vehicular platform that can offer extended operation in the infamous hypersonic flow environment. At speeds greater than Mach 5, the severity of aerodynamic heating exceeds the operational capabilities of most bulk materials traditionally used in mechanical design. Therefore, the development of novel hypersonic aircraft requires the integration of high performance insulative composites and cooling systems that can support continued exposure to hypersonic conditions [3,4]. Overcoming the challenges of hypersonic aerodynamics with a reusable system is highly desirable for many ultra-high speed aerospace applications such as rapid global transport and shipping [5], cost-effect low earth orbit payload delivery [6], and highly

responsive defence operations [2].

Aerodynamic heating is the combined result of specific aerothermodynamic fluid phenomena, such as viscous dissipation and convective shock wave heating, that become increasingly severe in proportion to the vehicles flight speed [7,8]. Mechanisms of aerodynamic heating are further aggravated by the sharp leading edges and slender airframe that characterise the design of hypersonic aircraft, allowing them to maintain high speed manoeuvrability and peak aerodynamic efficiency [5,9]. Considering the constant heat source imposed on the vehicle through structural integration of the scramjet engine [2], hypersonic airframes are exposed to a nonuniform thermal profile that consist of immense heat fluxes congregating around key regions of the aerostructure [5]. Lightweight, cost-effective and minimally invasive Thermal Protection Systems (TPSs) that function continuously in the hypersonic environment have subsequently become an urgent need for the practical development of airbreathing hypersonic aircraft. The design of hypersonic TPSs is a significant challenge as thermal protection must be provided within the stringent durability, weight, and reusability constraints required to maintain optimal vehicle functionality [10].

* Corresponding author.

E-mail address: elsa.antunes1@jcu.edu.au (E. Antunes).

Current methods of hypersonic thermal management rely on the integration of passive, semi-passive, or active-cooling mechanisms into the load bearing aerostructure itself. Externally insulated material layers, embedded heat pipes, and regenerative fuel cooling are key strategies of hypersonic TPS design currently under development [10, 11]. Active cooling is the most effective form of thermal management and has been shown to offer a high degree of thermal protection when exposed to even the most severe magnitudes of aerodynamic heat flux. However, it is parasitic TPS that impose hefty constraints on the weight, complexity, and cost of the overall aircraft design which hinder general practicality [12]. Although not as detrimental, alternative methods of passive and semi-passive TPSs also present parasitic characteristics such as poor manufacturability, difficult maintainability, and limited material availability that impact the hypersonic design feasibility [5]. The apparent flaws of existing TPSs emphasises a need for cost-effective insulative aerostructures that can withstand aerodynamic heating as a function of intrinsic material properties enhanced through optimal structural design. To maintain aircraft functionality, these structures must be lightweight with compressive load bearing capabilities alongside providing a high degree of insulation [10].

Mirroring some of the challenges presented by modern-day hypersonic vehicle design, sandwich structures rose to prominence in the aerospace industry as a design-level strategy of replacing solid titanium structures with cost-effective stainless steel alternatives during the development of early supersonic fighters and bombers in the United States [13]. The Mach 3 XB-70 "Valkyrie" pioneered an outer skin comprised of stainless-steel honeycomb sandwich panels that combined the mechanical strength and availability of common metals with a reduced relative density to maintain high speed aerial efficiency. Not only did these structures significantly reduce the weight of the entire aircraft, but provided a high degree of thermal insulation towards aerodynamic heating in the supersonic flow regime [14]. Honeycomb sandwich structures subsequently became a staple in the design of experimental aircraft that pushed the limits of aeronautical flight, such as in the famed Mach 2.2 "Concorde" passenger jet [15] and the fastest manned aircraft in the world, the Mach 3.3 SR-71 "Blackbird" [16]. Advancements in the fields of advanced manufacturing and material science have only improved the capabilities of contemporary sandwich structures through internal integration of complex architecture, such as periodic lattices, into specialized structures manufactured out of high-performance materials, such as technical ceramics. The historical precedent set by sandwich structures in relation to enhancing the performance of cutting-edge aircraft uniquely positions them to tackle the immense problem of hypersonic aerodynamic heating [10].

Current research into hypersonic sandwich structures has focused heavily on the combination of high temperature refractory metals or superalloys with synergistic core architecture that offsets their adverse bulk material properties such as inherent high densities and thermal conductivities [10]. Whilst the superior high temperature mechanical strength of these metals is valuable, their poor functional applicability as lightweight insulators in the extreme hypersonic environment has motivated investigations into better suited material alternatives [3]. Polymers and High-Temperature Polymer Composites (HTPCs) have been studied as the primary constituent in sandwich structure configurations for ultra lightweight, high temperature aerospace structures designed to improve the thrust-to-weight potential of rocket engines [17]. However, their poor high temperature durability limits their use to temporary TPS systems such as ablatives which are incompatible with the intended function of hypersonic aircraft [18,19].

Ceramics possess a suite of bulk material properties that are highly desirable in the design of lightweight, load bearing, insulative structures for aerospace applications including inherently low densities and thermal conductivities alongside high compressive strengths. However, characteristic brittle material properties been a limiting factor toward their adoption in many structural and dynamic applications [20]. Composite materials have become a mainstay in the modern aerospace

landscape due to their ability to overcome the unique limitations posed by bulk metals, ceramics, and polymers by combining them with a more mechanically or thermally superior constituent. Carbon fibre (C_f) based composites such as Carbon fibre Reinforced Polymers (CFRP) and Ceramic Matrix Composites (CMCs) are the most common type of composite materials used in high temperature aerospace applications due to the incredibly high thermal and mechanical capabilities of carbon [20,21]. CMCs have largely replaced traditional metallic and ceramic materials in the design of ultra-high temperature aerostructures as they offer a significantly higher strength- and stiffness-to-weight potential as well as improved oxidation resistance and thermal resilience as a result of the embedded ceramic matrix. Compared to conventional monolithic ceramics, CMCs offer the significant advantage of quasi-ductile deformation behavior which greatly improves overall toughness, damage tolerance, and flexural strength which make them far more desirable for structural applications [23,24].

Each class of high temperature materials offer unique structural characteristics that make them advantageous to the design of hypersonic aerostructures, especially when combined with the multifunctional enhancements gained through their integration in the form of a sandwich structure. The architectural design of a porous sandwich core governs its resultant effective material properties by altering the internal volume fraction of the structures bulk material [10]. It is therefore essential that the desired bulk material can be reliably manufactured into porous or cellular structures, an engineering challenge that has been streamlined by technological advancements in the field of Additive Manufacturing (AM). Ceramics have benefited immensely from the commercial introduction of AM as it offers the ability to accurately fabricate highly complex, near net shape solids that augment the bulk material properties for high thermal and mechanical performance in a number of sophisticated design fields such as medicine, automation, and aerospace [24,25].

Tunability, accuracy, and complexity are key characteristics of ceramic AM that make it a desirable avenue for the manufacture of hypersonic sandwich structures. Core porosity governs the effective material properties of sandwich structures, such that having direct control of pore size and unit cell wall thickness is an invaluable tool during design and development [10]. Furthermore, the integration of complex core architecture can provide further performance enhancements to the structure. For example, Triply Periodic Minimal Surface (TPMS) lattices have been shown to exhibit highly insulative thermal properties [27] and superior strength-to-weight ratios at low porosities [28], but the sheer complexity of their geometry requires the use of AM technology for practical production [29]. The direct topological and rheological control provided by AM-based design methodologies permits the use of advanced structural optimisation techniques, such as the introduction of functional gradients. Controlled topological gradients are known to provide an effective method of targeted functional optimisation over a structures volume [30]. Whereas emerging studies into functionally graded ceramics are identified as a promising strategy for improving the fracture toughness and flexural strength of the structure [31]. Despite these prominent advantages, ceramic sandwich structures often remain overlooked for structural applications due to crucial structural drawbacks including highly brittle failure, poor fracture toughness, and low impact resistance [32].

Amidst the current state-of-the-art hypersonic TPS design, research into the optimisation of sandwich structures is paramount to the successful development and production of airbreathing hypersonic aircraft. Although metallic sandwich structures currently dominate the field of study, research into ceramic sandwich structures has been ongoing and currently describes a range of structures uniquely equipped to offer incredibly lightweight, load bearing functionality with superior insulative performance [10,20]. As a result of being overlooked in favour of more conventional bulk materials, a comprehensive review into the design, materials, and performance of hypersonic ceramic sandwich structures as reported by current studies has yet to be conducted. The

scope of this review will therefore cover works investigating the design and evaluation of both monolithic and composite ceramic sandwich structures intended for use in ultra-high temperature hypersonic applications. In light of increasing private and sensitive governmental interest in this field of research, much of the current state-of-the-art is not publicly available [5] thereby limiting this review to focus on peer-reviewed advancements published by the academic community, which represents the extent of reliable public knowledge in the field of hypersonic design.

2. Hypersonic sandwich structures

Sandwich structures are a group of multilayered composites constructed by the “sandwiching” of an engineered core between two dense material layers, as described in Fig. 1. The internal core subsequently governs the performance of the structure as a function of material composition and topological design. Varying these parameters over the core volume provides a high degree of flexibility during the design process, allowing the fine-tuning of structural properties for high-performance applications [33]. For the purposes of this study, the term “sandwich structure” is analogous with structures composed of a topologically distinct core whose design extends to any given length scale by the repetition of a series of interconnected or freestanding geometries that can be defined on the basis of an individual unit cell [10, 33,34].

Hypersonic aerostructures are designed to be as lightweight and thermally resilient as possible while maintaining a suitable mechanical strength to withstand dynamic aerodynamic load conditions without material degradation [5]. As core architecture governs the material composition and structural integrity of the overall structure, topology optimisation of the cellular core becomes a crucial step in the development of high-performance hypersonic sandwich structures [26]. General dimensional definitions for a cellular sandwich structure are described in Fig. 1 over a strut-based pyramidal core configuration. Here, the top and bottom face sheets are coloured red and blue, respectively, to highlight the typical load scenarios of high-performance aerostructures [4]. Cellular core designs are topologically defined using the dimensions and characteristics of the unit cell that is repeated, either in a planar, array or periodic lattice configuration, throughout the core volume [35].

Given a homogenous material profile through the sandwich structure, the effective material properties become a function of the unit cell

geometry. For example, the relative density (ρ^*) of a cellular sandwich structure with homogenous material properties is determined by the volume of the face sheets (V_f) and the unit cell or core (V_c) relative to the bulk material density (ρ) as described using the equation: $\rho^* = \rho(2V_f + V_c)$. In the case of the pyramidal example provided in Fig. 1, the core volume is governed by the thickness (t) and length (l) of the struts used to construct the unit cell geometry [36]. With more complex unit cells, such as highly periodic lattices, it is more conducive to describe the relative density in terms of the bulk materials volume fraction within a unit cell of characteristic length, L , and height, H_c , as in Fig. 1 [37]. Additional geometric components of the unit cell play a role in characterising the mechanical response of the cellular core. In the ongoing example provided in Fig. 1, the inclination angle, ω , which denotes the angle of a unit cells strut relative to the face sheets, has been observed to have a significant impact on the specific strength and failure mode of a sandwich structure [38].

More importantly for the design of hypersonic aerostructures, cellular sandwich structures improve the passive insulation capacity of the bulk material, as the reduction of conductive material in the core correlates directly to a direct drop in the structure's effective thermal conductivity. The internal voids of the sandwich core also act as a versatile housing for the integration of additional solid insulation or active cooling mechanisms to improve thermal performance and increase the effective service temperature of the overall structure [10]. Whilst additional TPS integration can aid in managing the operational temperature of hypersonic aerostructures and distinct core topologies can be used to optimize crucial functional properties, the overarching performance remains limited by the capabilities of the bulk structural material. This section will outline some of the overarching core designs, methods of TPS integration, and high temperature materials studied in the wider field of research surrounding hypersonic sandwich structures. The importance of material selection and the scope of the current study will be defined in the latter stages of the section.

2.1. Materials

The severity of aerodynamic heating experienced by hypersonic aerostructures limits the applicable range of multifunctional materials that can satisfy the thermal, mechanical, and weight requirements of its structural design. Primarily, the material selection process considers the bulk materials melting point, thermal conductivity, oxidation resistance,

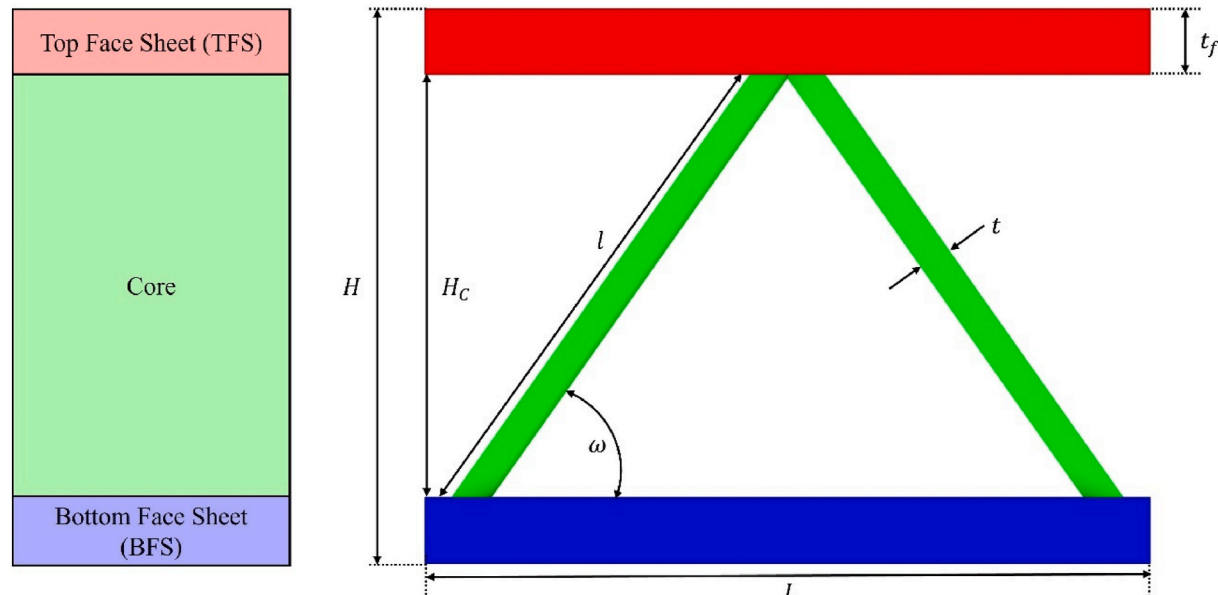


Fig. 1. Cellular sandwich structure design composition and general unit cell characteristics.

density, bending properties and compressive strength as the determinants of suitability. Oxidation resistance is a significant concern as gas ionization induced by ultra-high surface temperatures expedites oxidative material degradation and ablation due to plasma formation [39]. The chemical reactivity of the material or the suitability of applying protective coatings for oxidation protection must therefore be considered during material selection. Secondary mechanical properties that are of significance to the design and performance of hypersonic sandwich structures include flexural and bending strength, ductility, thermal shock resistance, and fracture toughness [5].

The most common materials studied in the wider literature include refractory metals, metallic superalloys, monolithic ceramics, CMCs, polymers, and CFRPs. Of these, refractory metals and superalloys have been the subject of significant investigative efforts due to their highly advantageous mechanical strength and ductility at high temperatures [10]. Specifically, refractory metals suffer from incredibly high densities and metallic superalloys require the use of expensive, difficult to apply Thermal Barrier Coatings (TBCs) to withstand temperatures greater than 1000 °C [40]. Moreover, metals possess inherently high thermal conductivities which prevent their effective use in an insulative capacity without additional thermal management [5].

Monolithic ceramics are sought after for their comparatively low densities, very low thermal conductivities, and superior mechanical strength. Although sparking the interest of researchers, work in this area has been dissuaded by the traditional drawbacks of monolithic ceramics that have limited their applicability towards dynamically loaded structures. Current studies instead focus on the use of high-performance CMCs which combine the desirable thermal characteristics of monolithic ceramics with the superior mechanical strength and ultralight-weight density properties of fibrous reinforcement [20,40]. Most notably in comparison to their monolithic counterparts, CMCs have been shown to elicit quasi-ductile failure behaviour that provides a much higher overall toughness with superior damage tolerances, energy absorption, reduced susceptibility to crack propagation, and far superior flexural capabilities under dynamic load conditions [23]. Carbon fibre reinforcement of a Silicon Carbide (SiC)-based ceramic matrix is one of the most common CMC configurations used in hypersonic aerostructure design as it provides significant high temperature oxidation and ablation resistance as a result of the SiC matrix [5]. Polymers and CFRPs are far more susceptible to heat than both metallic and ceramic materials but are incredibly lightweight with impressive ranges of plastic deformation, fracture resistance, and ductility. For the purposes of hypersonic design, these lower temperature materials are mostly designed to function as lightweight core structures in ablative TPSs [41]. The materials selection is a crucial step in the design process of a hypersonic sandwich structure, as the primary structural constituent will define the governing bulk material properties of the structure, available methods of manufacture, subsequent design complexity, and determine whether the integration of additional TPS mechanisms is necessary [5].

2.1.1. UHTCs

Compared to polymeric and metallic materials, ceramics possess a suite of promising characteristics for insulative aerostructure applications such as very low thermal conductivities and excellent compressive strengths. These desirable characteristics are even more pronounced in Ultra High Temperature Ceramics (UHTCs), a class of borides (B), carbides (C), and nitrides (N) of early transition metals such as Zirconia (ZrO_2), Hafnium (HfO_2), Tantalum (Ta), Titanium (Ti), and Niobium (Nb). UHTCs are classified by their capacity to maintain chemical stability at temperatures greater than 2000 °C [20]. Whilst the applicability of many conventional technical ceramics in the context of hypersonic design is limited by the sheer extremity of its aerothermodynamic operating environment, UHTCs make ideal aerostructure design candidates as they able to withstand temperatures in excess of 3000 °C without material degradation. As a byproduct of their high temperature resilience, they also exhibit excellent thermal shock and wear resistance,

hardness, and high thermomechanical strength [21,42]. However, their high temperature characteristics also makes UHTCs a difficult class of ceramics to process and manufacture, as the large sintering parameters and additives used to achieve densification often significantly influence the mechanical properties and microstructure of UHTC structures. UHTCs are therefore much more expensive to prepare for structural applications compared to conventional technical ceramics, and the difficulty of their production limits component scalability [43,44]. As a whole, the suitability of all classifications of monolithic ceramics for dynamically loaded aerostructures is encumbered by their infamously brittle fracture mechanics, limited flexural capacity, and poor impact resistance [21].

Monolithic and composite UHTCs provide an important platform for the development of ultra-high temperature hot structures in hypersonics. Hot structures must resist oxidised aerothermodynamic heating at temperatures that can exceed 2500 °C without the use of thermal management, such as leading edge geometries and acreage airframe skins [5,9]. Zirconia Diboride (ZrB_2), Zirconia Carbide (ZrC), Hafnium Diboride (HfB_2), and Hafnium Carbide (HfC) have been the subject of significant research efforts into hot hypersonic structures as they have superior high temperature chemical stability and mechanical strength retention alongside advantageous thermal conductivities [3,42,45,46]. Although ZrC and HfC offer a service temperature above 2000 °C due to increased melting points [39,47], ZrB_2 and HfB_2 offer superior oxidation and ablation resistance [42,48]. The combining of ZrB_2 and HfB_2 with SiC has been thoroughly investigated for hypersonic design, as these composites are found to improve the oxidation resistance of the structure compared to their monolithic constituents [49–52]. SiC further improves microstructure refinement during UHTC densification to simplify manufacturing and, in the case of HfB_2 -SiC composites, offers a reduction in thermal conductivity [53,54].

UHTC manufacture is a challenging process due to the strong atomic bonding and low diffusion that provides their superior high temperature material properties. High part densification is subsequently not achievable with conventional pressureless sintering mechanisms, and pressure-assisted processes such as Hot Pressing (HP), Hot Isostatic Pressing (HIP), or Spark Plasma Sintering (SPS) are recommended [39, 55,56]. Pressure-assisted sintering methods are generally more expensive than pressureless processes as a result of the apparatuses used to provide high temperature compression and the required fabrication of consumable dies for net shape fabrication. Moreover, HP and SPS methods can only produce simple part geometries that must be post-processed to achieve higher complexity structures. This is particularly problematic for UHTCs with high hardness, as extensive diamond grinding or electrospark wire-electrode cutting would be required to achieve a final part design [20,57]. The challenges and limitations associated with UHTC densification have thus far prevented significant investigation into the topological optimisation of their impressive material properties through the use of cellular networks and complex structures [39]. However, emerging methods of UHTC specific AM based on the processes of Direct Ink Writing (DIW) [58,59] and Select Laser Sintering (SLS) [60,61] provide a tentative glimpse into the inevitable future of net shape UHTC manufacture. The refinement of these methods is expected to further promote research into cellular ceramic sandwich structures with bulk UHTC material properties leading to further performance enhancements for multifunctional hypersonic aerostructures.

2.2. Architectural design of the porous sandwich core

Sandwich structures are optimized for maximum performance in many multidisciplinary applications mainly through parameterization of the core design. Solid structures are governed by the bulk material properties of their primary structural constituent, whereas sandwich structures utilise different solid compositions and repeating microstructural geometries to tailor these properties for specialized applications [33]. There is an incredibly diverse range of core topologies that

offer unique characteristics when enclosed in a sandwich structure, with Fig. 2 displaying some of the overarching core architecture classifications used in the specific development of ceramic sandwich structures for high temperature applications [34].

Traditional planar core sandwich structures, such as those with corrugated and honeycomb core configurations, are designed to minimise the system's weight while maintaining a high strength-to-weight ratio. The continuous core struts provide high compressive and flexural strength under dynamic load which has led to the widespread adoption of planar sandwich cores in the in the aviation industry [13]. Folded cores are a more modern configuration inspired by origami, providing a high degree of stiffness, bending strength and twisting resistance due to their unique force redistribution and energy absorption characteristics [62]. In lieu of a structured core topology, foam-core sandwich structures are manufactured using highly porous materials or interconnected strut-based networks with random connections to improve the designs thermal and acoustic insulation capabilities [63].

Array-based and periodic lattice architectures describe a range of complex core topologies with extremely high porosity tolerances. As a result of sheer complexity (Fig. 2), periodic lattice cores have only become prominent in engineering design following significant technological advancements in the field of AM which has allowed their reliable manufacture [25]. Periodic lattices refer to an incredibly diverse range symmetric unit cells that are periodically layered and patterned to form a larger, interconnected cellular network [64]. Comparatively, array configurations employ the use of asymmetric, truss-based unit cells repeated along a single axis through the sandwich core. Both core variations possess low relative material densities due to innately high porosities, allowing for superior lightweight potential and high strength-to-weight ratios. Compared to simpler core architecture, the high porosity of periodic and lattice core topologies offer significant improvements to a sandwich structures insulation [26]. However, despite the performance enhancing characteristics of sandwich structures, they are still limited by the bulk material properties of their

primary structural constituent. As the severity of aerodynamic heating imposed during hypersonic flight exceeds the operating limits of most readily available structural materials, it is important to consider the feasibility of integrating additional mechanisms of thermal management into the structural design [65].

2.3. System-level integration

The multifunctionality of cellular sandwich structures provides a degree of flexibility to their integration in a given hypersonic system. In their base configuration, these structures are designed to provide a lightweight, load bearing platform that offers passive thermal protection in the form of reduced heat transfer through the sandwich core. A multifunctional structural profile such as this is well suited for general external airframe or skin applications in the form of a passive acreage TPS [66]. However, the thermal load induced by aerodynamic heating is not uniform over a hypersonic airframe with specific areas of the structure being subjected to excessive thermal loads that could not be adequately compensated for through a passive insulation mechanism [12]. Therefore, additional methods of thermal management can be integrated into the porous core architecture of cellular sandwich structures to improve localised thermal protection for locations of excessive heat accumulation such as leading edges [67], or to provide additional insulation for sensitive system components like the electrical control system [68]. Moreover, the versatility of cellular sandwich structure design can provide the basis for functional grading of various integral TPS systems throughout an airframe for localised thermal protection, reducing design redundancy in terms of excess material expenditure, weight, and coolant consumption.

TPS integration into the load bearing structure of a hypersonic aircraft is considered the most practical strategy of bolstering overall thermal protection. The literature describes three overarching TPS configurations that are integrated into hypersonic sandwich structures, classified in this study as hot, insulated, or actively cooled as illustrated

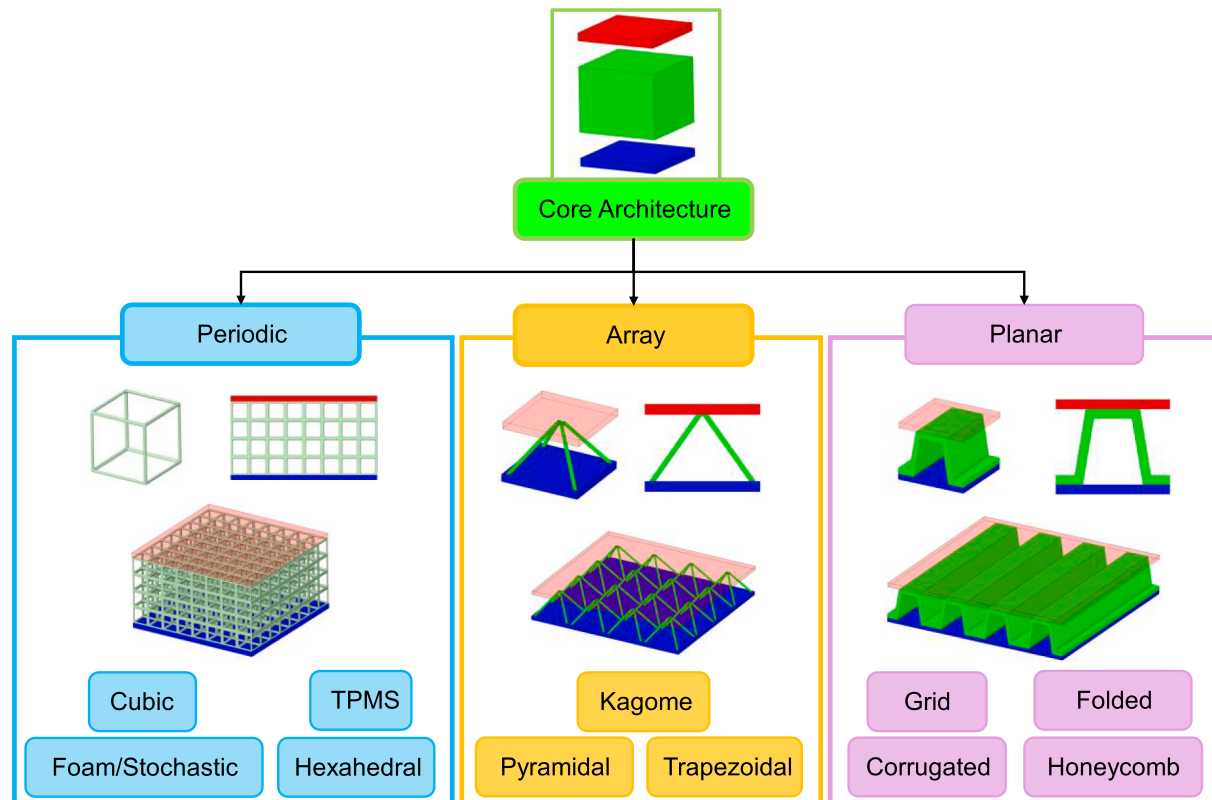


Fig. 2. Core architecture classifications.

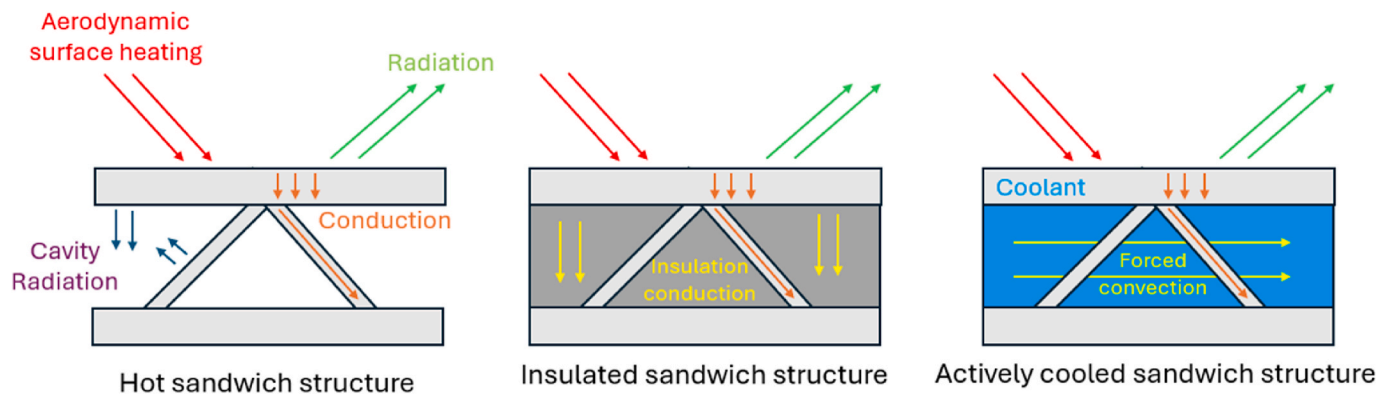


Fig. 3. Ceramic sandwich structure TPS configurations.

in Fig. 3 alongside their corresponding mechanisms of heat transfer.

Hot sandwich structures do not possess any form of integrated TPS and rely on passive radiative heat transfer to the ambient environment to achieve thermal equilibrium with incoming aerodynamic heating and insulate the vehicle's interior [5]. Although being the most cost-effective, simple, and lightweight configuration for a hypersonic aerostructure, hot structures have stringent material requirements and must be perfectly optimized to prevent failure. The porous nature of the core reduces the overall effective thermal conductivity of the structure relative to its bulk material properties for reduced heat transfer, but it also introduces radiative heat transfer between differentially heated surfaces in a phenomenon known as cavity radiation. This can become problematic if the internal temperature gradient becomes too high and cavity radiation becomes the dominant mechanism of heat transfer over thermal conduction [36]. Alongside their applicability as external skins over the airframe, hot structures can be used to replace most dense structures in the aircraft for further weight reductions given suitable optimisation of their effective mechanical properties.

Insulated sandwich structures incorporate additional, heat-resistant materials into the voids of the porous core to provide an additional layer of thermal protection. The internal material both eliminates the risk of cavity radiation to ensure conduction remains the dominant mechanism of heat transfer throughout operation as well as providing mechanical reinforcement to the core architecture. Although becoming the subject of numerous numerical investigations, the extreme manufacturing difficulties associated with the implementation of internal insulation has thus far prevented extensive experimental testing of these sandwich structure configurations. Furthermore, the extreme operating environment of hypersonic aviation precludes the use of all but the most temperature resistant insulation materials to become effective and offset the additional cost, complexity, and weight [10]. Nonetheless, the design of insulated cellular sandwich structures can be a powerful tool to efficiently control heat transfer and provide cost-effective thermal safety nets in heat sensitive areas such as manned crew quarters, electrical control surfaces, and fuel tanks [68].

Actively cooled structures are the most effective form of sandwich structure-based TPS configuration and benefit from the use of internal porosity as intrinsic cooling channels. By utilising a recirculating coolant such as the aircraft's fuel source, the porous core becomes a channel for the forced convective heat transfer of incoming heat away from the sandwich structure to efficiently maintain its core temperature. Cooled structures have been tested to reliably withstand even the most severe thermal loads projected to be experienced by airbreathing hypersonic vehicles and provide such an effective degree of thermal management that cost-effective, low temperature structural materials can be used without risk of thermal failure. Although fundamentally satisfying the thermal requirements of hypersonic aviation, actively cooled sandwich structures are not feasible for general use due to the cost of integration, complexity, and weight of the cooling subsystems [12,66]. However,

their integration into a sandwich structure configuration reduces the burden on design by removing the need for dedicated cooling channels and heat pipes. Whilst still problematic for general thermal management, actively cooled TPS configurations have proven to be invaluable for the thermal management of structural locations experiencing the maximum thermal load of the hypersonic environment such as leading edges of the airframe [67] and scramjet combustors [69].

2.4. Comparison with current literature reviews

Only a limited number of reviews have been conducted into the design of optimized sandwich structures for hypersonic or high temperature aerospace applications due to the specialized nature of the research field. The small selection of studies that have been undertaken are collated in Table 1 alongside indicators of their scope including materials, architectural design of the sandwich core, and methods of TPS integration.

Kausar et al. [70] investigated the state-of-the-art manufacturing methods and technologies used to fabricate metallic, polymer, and composite sandwich structures with simple core topologies. This review reported that the manufacturing method used for the fabrication of high-performance sandwich structures is dependent on the bulk materials, face sheet and core design required to optimize the material properties for the desired application. Karsandik et al. [71] studied the impact behaviour of metallic and composite polymer sandwich structures with foam and honeycomb core topologies intended for conventional aeronautical applications. It is found that alongside core material, design, and face sheet thickness, the orientation and architecture of fibres in the face sheet play an important role in determining impact resistance and damage tolerance of composite sandwich structures. Liu et al. [64] reviews the current state of research into the active cooling of metallic and polymeric sandwich structures with simple and complex core geometries intended for use in hypersonic applications. This study identified key limitations associated with current methods of additive manufacturing for porous and lattice core metallic sandwich structures, particularly in the porosity control and size uniformity of resultant core architecture. This has resulted in most of the research surrounding actively cooled hypersonic sandwich structures relying on numerical and mathematical modelling.

Sajjad et al. [26] reports advancements in the use of periodic lattice structures for a variety of thermal systems, including hypersonic thermal protection, and assesses all target materials and active cooling mechanisms. This review confirms lattice structures greatly reduce the weight and increase the mechanical strength of comparable thermal systems; however, their exact thermo-mechanical properties are dictated by the design of the lattice architecture itself. Feng et al. [34] provides a comprehensive review on state-of-the-art topological core designs and their influence on the performance of general sandwich structures without specific reference to a particular field or industry. They

Table 1

Scope and relevancy of prior reviews into sandwich structures.

Ref.	Year	Materials			Core Architecture			TPS Configurations		
		Metals	Polymers	Ceramics	Periodic	Array	Planar	Passive	Insulated	Active
[10]	2021	✓	✓	✓	✓	✓	✓	✓	✓	✓
[64]	2022	✓	✓		✓	✓				✓
[70]	2023	✓	✓				✓	✓	✓	
[71]	2023	✓	✓				✓	✓		
[26]	2022	✓	✓	✓	✓	✓		✓		✓
[73]	2021	✓	✓		✓	✓	✓	✓	✓	
[34]	2020	✓	✓	✓	✓	✓	✓	✓	✓	
[74]	2020	✓	✓	✓	✓			✓		✓
[13]	2020	✓	✓				✓	✓	✓	
[75]	2019	✓	✓				✓	✓	✓	
[76]	2019	✓	✓	✓			✓	✓	✓	
[33]	2018	✓	✓	✓	✓	✓	✓	✓	✓	
Current	2025			✓	✓	✓	✓	✓	✓	✓

conclude that the geometric influence of sandwich structure design on the loaded response and effective material properties creates an inherently multifunctional structure of which its performance can be tailored for any number of advanced applications and environments.

Le et al. [10] is the most similar review to the work conducted here with a much larger scope, collating all reported works of sandwich structures in hypersonic thermal protection regardless of material or TPS configuration. The bulk of work collated in this study involves metallic and composite sandwich structures, however the advantages of CMCs in terms of high temperature resistance and structural strength are found to be superior by comparison. The practicality of these advanced composites is hindered by the costs of development, manufacture, and *in-situ* testing. Le et al. [10] predicts that advances in additive manufacturing will improve the practicality of such structures by easing the development process and allowing more extensive performance assessment of prototypes including fatigue, impact, and vibrational analysis.

Pan et al. [72] investigates methods for the design and optimisation of metallic, polymer, and ceramic lattice structures for a variety of applications including aviation. The primary conclusion of this report emphasises the importance of individual unit cell topology in dictating the final thermal and mechanical properties of the full lattice structure. Birman and Kardomateas [33] provide a comprehensive review on the current state-of-the-art sandwich structure design methodologies in consideration of a wide range of materials, topologies, and configurations for several applications including high speed aerospace design. The result of this review identifies the challenge of modelling sandwich structures in three-dimensions, particularly in reference to modelling unique phenomena, geometric anomalies, and multi-material interactions resulting from the inherent multifunctionality of sandwich structure designs. Birman and Kardomateas [33] also discuss the rapidly evolving landscape of sandwich structure design with new concepts being constantly explored due to their versatility. The introduction of functionally graded core architecture is a key example of ongoing developments in the research field, allowing for more precise tailoring of the structural response, enhanced toughness, and improved resistance against face sheet debonding.

The present study investigates current state-of-the-art design of ceramic sandwich structures optimized for load bearing, insulator applications in hypersonic aircraft and ultra-high temperature applications. Compared to prior reviews, the present work limits the literature review to investigations involving structures designed using monolithic ceramics and their composites regardless of architectural core design or TPS configuration. Key discussions in this review will focus on material trends in terms of ceramics and CMCs, current methods of manufacture, analysis techniques and models, the unique characteristics of different core architecture, and the integration of unique TPS mechanisms.

3. Ceramic sandwich structures

The following section outlines the current state-of-the-art development of ceramic sandwich structures including manufacturing and material trends, core designs, and methods of TPS integration. Whilst conventional sandwich structures have been used in aeronautical and astronautical design since the early 1960's [10,13], the incorporation of ceramics to improve thermal resistance is a relatively new field of research. Fig. 4 provides a quantitative breakdown of publications per year, beginning with a technical brief authored by NASA that describes the development of an integrated TPS using a Ceramic Matrix Composite (CMC) in 2009. The report describes the manufacture of a foam-core sandwich structure using a Carbon fibre reinforced Silicon Carbide (C_f/SiC) fabric [77].

As described in Fig. 4, studies into ceramic sandwich structures for high temperature applications reached a gradual peak between the years 2017 and 2019 but have since been in steady decline. This trend indicates contrasting views on the research field's future, but further context can be gleaned through analysis of the country of origin for the bulk of reported work in Fig. 5.

An overwhelming portion of current research has originated in China with 72 % of reported studies being published by scholars from Chinese institutions as illustrated in Fig. 5. The remaining 28 % is comprised of European, Australian, and North American institutions with the latter only making up 2 % of total reported studies in spite of the USA's extensive history of aerospace innovation [1,13]. Therefore, it can be hypothesised that such a distribution does not accurately reflect the quantity of research being conducted by western countries, particularly in the case of the USA as evidence of hypersonic progression can be observed through the testing of several prototype hypersonic aircraft [4, 9]. However, given rising private and military interest in the successful development of such vehicles, a significant portion of research is assumed to be confidential or proprietary and is therefore not publicly accessible [5]. For example, a report published in 2015 by Goodman et al. [78] discusses the successful manufacture of a C_f/SiC honeycomb sandwich structure using a proprietary AM process. This report claims that the structure exhibits a near-zero Coefficient of Thermal Expansion (CTE) making it particularly applicable to the design of high temperature sandwich structures and insulators. The subsequent lack of publicly available follow up research suggests that further development of CMC-based honeycomb sandwich structures may have been privatized for subsequent commercial development. Such a precedent has been set in the past during the secretive development of high-performance military aircraft such as the SR-71 "Blackbird" by private defence contractors [16].

Furthermore, the decline in research, particularly depicted in Fig. 4 can also be attributed to the rising interest in UHTCs for hypersonic applications [20]. As the technology to reliably fabricate UHTCs and

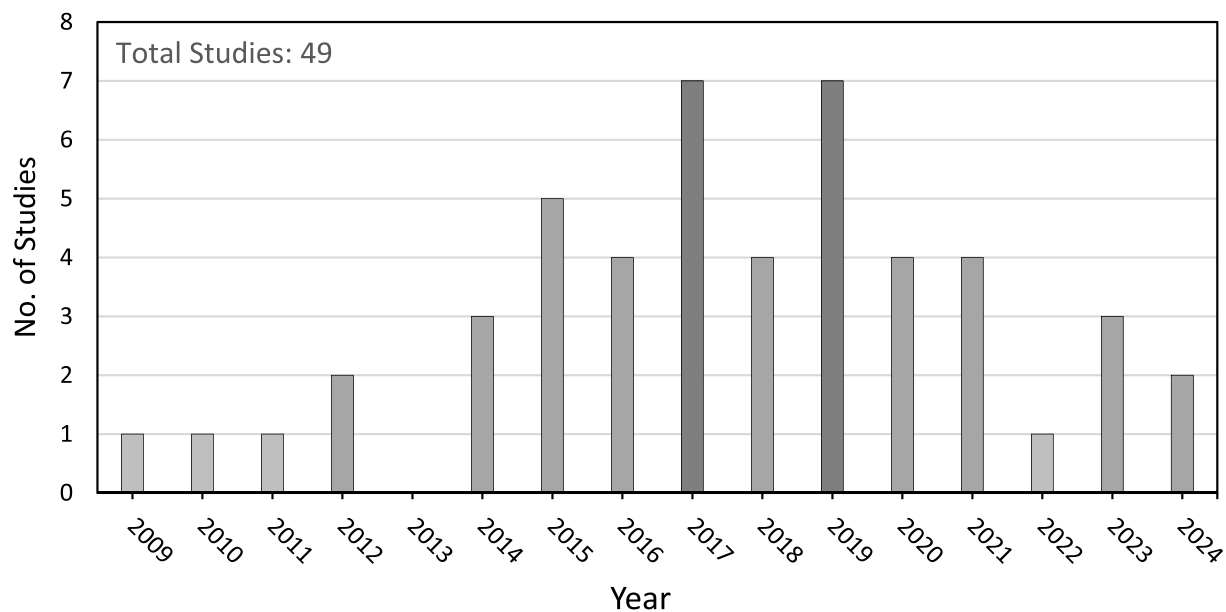


Fig. 4. Number of reported studies into ceramic sandwich structures per annum.

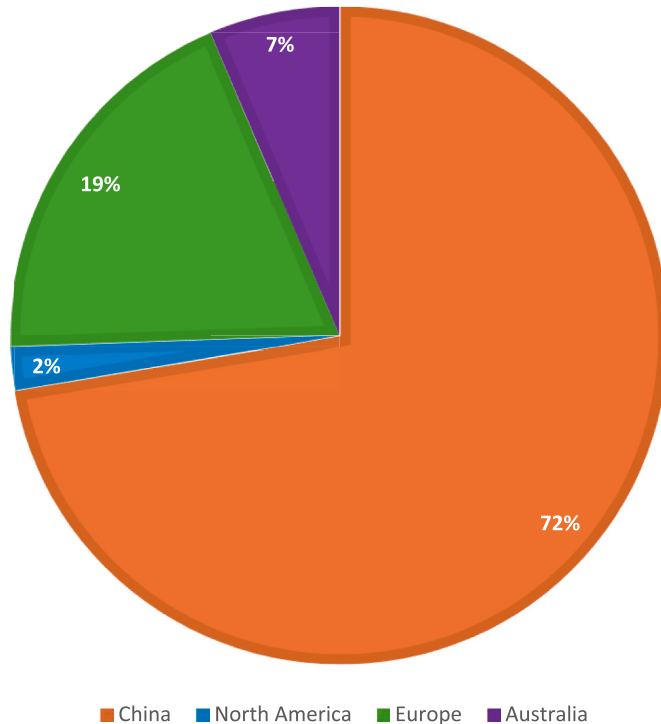


Fig. 5. Breakdown of total studies per country.

their related composites with the complexity required of cellular sandwich structures has yet to be established, research into their hypersonic application has primarily focused on ultra-high temperature material characterisation [46], composite development [21], and refinement of manufacturing procedures [79]. Given the prevalence of CMC sandwich structure development reported in the literature, the future development of UHTC cellular sandwich structures can be assumed with near certainty. However, the current state-of-the-art only possesses a handful of investigations into UHTC structures, specifically ZrB_2 [59] and a ZrB_2 - SiC -C composite [57].

3.1. Materials

The distribution of specific ceramic materials in the literature is illustrated in Fig. 6 with some of the standard material properties most relevant to hypersonic design provided in Table 2. Current research suggests that the use of CMCs, particularly C_f/SiC as it accounts for over 55 % of currently reported work, has become the standard configuration for the investigation and proposal of hypersonic ceramic sandwich structures (Fig. 6). Despite its recent conceptualization, C_f/SiC has become a prominent structural material in the aerospace industry following the continually increasing thermal requirements associated with emerging propulsion, aeronautical, and astronautic technologies. Internal carbon fibres increase the flexural strength and fracture resistance of the composite such that it exhibits near ductile mechanical behaviour. Both fibre and matrix materials possess very low bulk densities and, although not being the most temperature resistant technical ceramic, Silicon Carbide (SiC) still possesses a desirable thermal

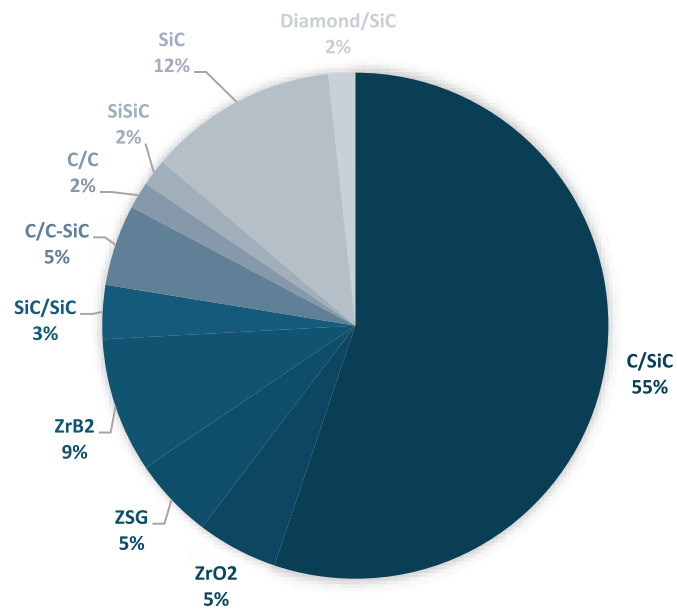


Fig. 6. Material distribution in studies of ceramic sandwich structures.

Table 2

Bulk properties of materials reported in studies of ceramic sandwich structures.

Material	Density (cm. g ⁻¹)	Melting Point (°C)	Service Temperature (°C)	Thermal Conductivity (W.(m.K) ⁻¹)	Coefficient of Thermal Expansion (10 ⁻⁶ .K ⁻¹)	Ultimate Strength (MPa)	Youngs Modulus (GPa)	Refs.
SiC	3.3	2800	1600	80@RT ^a	2.2RT 4@1000 °C	230-825	207-483	[37, 80]
SiSiC	3.1	1380	1350	120-200@RT 40@1000 °C	3.9	300	350	[81]
SiC _p /SiC	2.67	2800	1500	—	—	—	—	[82]
SiC _f /SiC	2.3-2.4	2800	1600	—	4	—	—	[23]
C _f /SiC	1.6-2.1	2800	1600	9.34-14.5@RT 4.49@1500 °C	2@RT-1500 °C	198-312	70-111	[23, 83]
C/C-SiC	1.9-2.3	2800	1600	9-18@200 °C 7.5-12.4@1650 °C	1.1@100 °C 4.4@1400 °C	80-190	50-60	[23, 83]
C/C	1.6-1.98	3650	1800	52@RT	—	98-235	395	[84]
ZrO ₂	5.6-6	2700	1000	2@RT	5.7	800-2000	240	[80, 85]
ZrB ₂	6.1	3245	1400	60@RT 55@2200 °C	6.2	438-458	489	[42]
ZrO ₂ -SiC-C (ZSG)	4.49-5.5	—	1600	84.7@RT 41.8@2000 °C	—	345-471	—	[57]
Diamond _f /SiC	3-3.1	—	1600	180-417@RT	—	185.9	—	[86, 87]

^a Room Temperature (RT).

conductivity with an appreciable melting point.

Although alternative fibrous SiC-based CMCs have been investigated, such as C_f/C-SiC [88] and SiC_f/SiC [67], none have provided the degree of balance between thermal and mechanical performance as C_f/SiC [23]. Particulate reinforcement has been explored by Zhang et al. [82] and Tang et al. [86] using both SiC and diamond particles, respectively. Whilst SiCp/SiC is not reported to exceed the mechanical performance of C_f/SiC, its compatibility with modern AM techniques is a unique structural advantage. Conversely, the Diamond_f/SiC sandwich structures manufactured by Tang et al. [86] are observed to possess a much higher intrinsic hardness and compressive strength compared to similar carbon fibre reinforced structures. Moreover, they retain a larger degree of mechanical strength at higher temperatures but suffer from higher effective thermal conductivities and are noticeably more brittle. The need for inherent high temperature oxidation resistance is evident by the presence of SiC in 84 % of the reported studies. Unlike alternative materials that rapidly degrade under high temperature oxidation, SiC reacts in oxygen-rich environments to form a Silicon Oxide (SiO₂) film over the exposed surface, protecting the underlying substrate from oxidation ablation. The protective qualities of SiC are particularly important for CMCs due to the high ablation susceptibility of carbon under oxidised conditions at temperatures as low as 400 °C [23].

Monolithic Ultra High Temperature Ceramics (UHTCs) and high temperature technical ceramics have been unexplored outside of a handful of investigations into the use of Zirconium Oxide (ZrO₂) and Zirconium Diboride (ZrB₂) structures. The compressive strength and insulative performance of Zr-based ceramics exceeds the performance of alternative Si-based ceramic and CMC sandwich structures [80], however preliminary fracture of the internal trusses or supports remains a primary concern and is one of the driving forces towards the mass adoption of CMCs in these applications [89]. Studies into Zr-based sandwich structures have therefore moved their focus onto ZrB₂ which has been shown to provide better oxidation resistance at the cost of being more difficult to manufacture because of exceedingly high sintering requirements [50].

ZrB₂ possesses oxidation characteristics akin to SiC, whereby a protective layer of Diboride Trioxide (B₂O₃) forms in heated oxidative environments to protect the ZrB₂ substrate from degradation at temperatures up to 1400 °C [90]. Wei et al. [57] hypothesise that a composite consisting of ZrB₂, SiC and Graphene would provide an improvement to the service temperature and mechanical strength compared to their individual monolithic components. A prototype Zirconia, Silicon Carbide, and Graphene (ZSG) corrugated sandwich

structure was manufactured using a material composition of ZrB₂-20 vol % SiC- 15 vol% G. Empirical heat transfer testing highlights the formation of three distinct oxidation layers at a test temperature of 1600 °C, protecting the composite from high temperature degradation. These observations are consistent with research suggesting that ZrB₂-SiC composites remain stable up to temperatures in excess of 1700 °C [42,90,91] and it was proposed that a ZSG composite has the potential to offer a service temperature greater than 2000 °C [57].

Standard properties for materials currently used in the development of hypersonic cellular ceramic sandwich structures are provided in Table 2. It should be noted that the material properties for CMC and composite ceramics are only approximate estimates, as the effective properties of these composites are dependent on a wide variety of factors such as fiber orientation, matrix composition, and preparation method [88]. Of particular significance to the design of cellular ceramic sandwich structures is the Coefficient of Thermal Expansion (CTE). In the case of non-homogenous sandwich structures with bonded cores such as CMCs, maintaining a matching CTE between the core and face sheets is paramount to preventing expansion stresses and crack initiation on the face to core joints during thermal loading [92,93] or preventing delamination during the densification stages of manufacture [93]. For ceramic materials in general, a higher CTE increases structural damage and crack propagation due to thermal shock. The high-speed nature of hypersonic aviation elicits a wildly nonlinear aerodynamic heating profile over a vehicles airframe, therefore subjecting the underlying structural material to intense cyclical thermal loading [5]. Therefore, selecting a material or material composition with minimised and matching CTEs is paramount to preventing expedited fatigue build up, thermal shock induced crack propagation, and material wear as a result of rapid volumetric changes of the structure [77].

3.2. Methods of manufacture

The manufacturing methods currently employed to fabricate prototypical ceramic sandwich structures for experimental analysis can be evaluated on their capability to produce high quality test specimens of varied complexity. Although utilising distinct processes, the manufacture of both CMC and conventional ceramic structures can be categorized by two similar production stages: preforming and densification. The methods of preforming and densification reported in the literature for the fabrication of cellular ceramic sandwich structures will be discussed in the following sections alongside a review of reported sandwich component bonding mechanisms.

3.2.1. Preforming

In the production of CMCs, preforming refers to the net shape construction of a C_f or CFRP preform for subsequent infiltration and embedding of the ceramic matrix. Generally, the preform lay-up process for initial C_f preform production involves the arranging of carbon filaments in conjunction with prefabricated, often interwoven, C_f panels. Wei et al. [94] utilises this procedure for preforming of an array core topology, with small cylindrical molds utilised to ensure even interweaving of C_f bundles into pyramidal unit cells whilst maintaining face sheet parallelism. Subsequently, a thin pyro-carbon layer was deposited over the sandwich preform by Chemical Vapor Deposition (CVD) at 960 °C with a propane (C_3H_6) precursor. The preform was then subjected to a graphitisation treatment at 1800 °C in Argon to achieve a weak interphase prior to the Chemical Vapor Infiltration (CVI) of the SiC matrix.

A different variation of this procedure was developed by Song et al. [95], whereby the face sheets, constructed using 6 layers of carbon-fabric cloth layers with 12k C_f tows infiltrated with polycarbosilane, were laid into a steel mould which provided a jig for the drilling of precise holes that allowed stitching of the pyramidal unit cells with continuous towpreg. The stitched preform was pressurised at 0.3 MPa in an autoclave and heated to 120 °C for 180 min and then 150 °C for 180 min to achieve cross-linking solidification of the face sheets and stitched core. Drilling through the face sheets for C_f stitching undoubtedly has an impact on the structural integrity of the face sheets as evident in the face sheet fracture reported by Song et al. [95] during out-of-plane compression testing.

This procedure was also employed by Yang et al. [96] bonding of trapezoidal unit cells in an C_f/SiC array core sandwich structure. An automatic tailor machine was instead used to cut core precursors out of 3-layer woven carbon fabric cloth with 12k C_f tows infiltrated with polycarbosilane. The precursor is then bent to resemble the desired unit cell and the placed in a metallic mould for attachment to the face sheets using 4-layer woven carbon-fabric cloth infiltrated with polycarbosilane. Chen et al. [97] fabricates a corrugated preform using a five layered T700 C_f tow laminate infiltrated with polycarbosilane. The laminate was placed into a metal die of the corrugated core geometry and pressurised under a vacuum to bond the sandwich components via crosslinking. Although this method is a relatively streamlined method of preform fabrication, the resultant corrugate sandwich structure exhibited consistent catastrophic failure in the form of intralayer delamination

and debonding during mechanical testing.

Heidenrich et al. [88] describes the construction of $C_f/C-SiC$ sandwich structure CFRP preforms by assembling C_f/C plates with equidistant slits cut into their cross-section via laser cutter. The plates could then be physically interlocked to create the grid core topology. The C_f/C core was joined to the C_f/C skins to create the preform sandwich structure using a carbon-based joining paste with each face sheet left to cure at 220 °C for 4 h. Whilst this method of C_f/C layup has its advantages in the form of fabrication speed and control over fibre alignment in the core, the reliance on stiff plates for core construction limits the topological potential of the cellular sandwich structure design.

Fig. 7 provides an overview of the manufacturing processes described in the literature for the prototypical fabrication of monolithic and composite ceramic cellular sandwich structures, including both traditional casting techniques and more advanced AM methods. Corrugate ZrO_2 sandwich structures manufactured by Wei et al. [85] via gel-casting using a 3Y- ZrO_2 slurry with 50 vol% solid loading. Gel-casting is a net shape process that involves the mixing of ceramic powders with organic monomers into a suspended aqueous slurry for polymerisation in a nonporous mould. The slurry hardens to form a green body that must be densified via a sintering stage [98]. Geometrical anomalies are observed in their gel-casted test specimen including a perceived waviness in the face sheets and irregular thickness of the core trusses (anomalies can be observed Table 4).

Contemporary AM technology has provided effective methods of circumventing bottlenecks associated with traditional ceramic manufacture and provides the capacity to investigate part geometries of a significantly higher complexity [25]. Select Laser Sintering (SLS) is a powder bed fusion manufacturing process that utilises a high intensity Carbon Dioxide (CO_2) laser to sinter selective, preheated layers of a powdered ceramic. The high intensity laser both densifies and sinters the material during printing, increasing the speed of production and allowing near complete part densification [99]. Mei et al. [100] reports the high degree of accuracy afforded by SLS which allows the manufacture of SiC test specimens with complex, multilayered BCC core topologies. Resultant experimental test specimens presented smooth face sheets and straight internal trusses, streamlining the subsequent sol-gel process used to integrate a Quartz fiber reinforced Silicon Oxide (Q_f/SiO_2) aerogel for additional insulation.

DLP is a variation of vat-polymerisation that utilises a high-power Ultraviolet (UV) light source to cure entire layers of resin, providing a

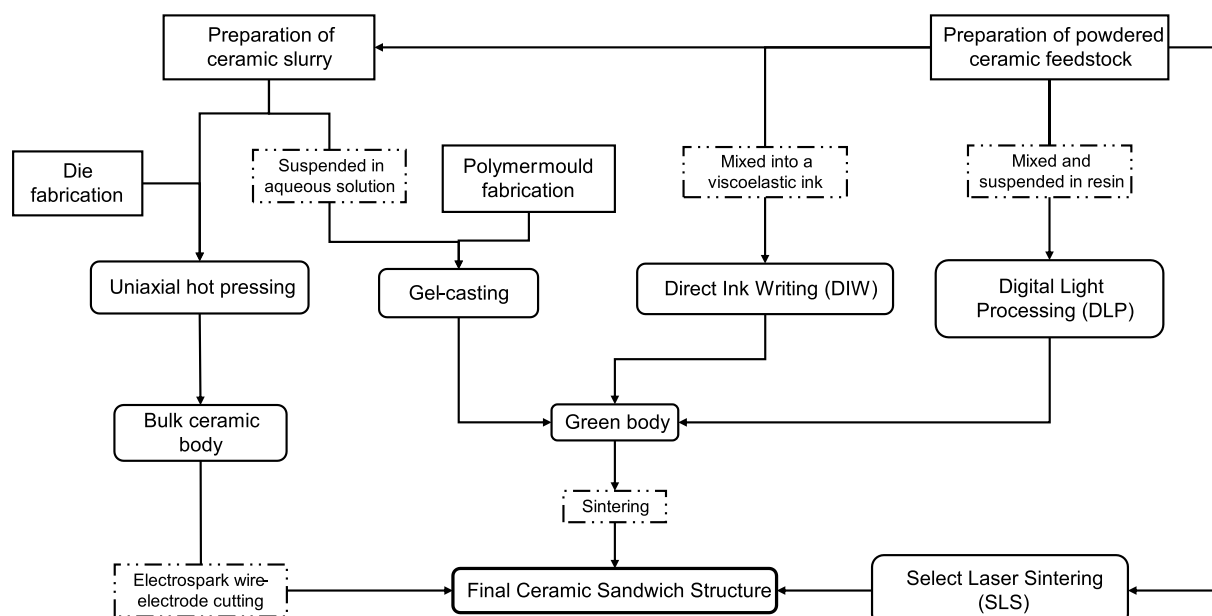


Fig. 7. Forming procedures used in the manufacture of ceramic sandwich structures.

high degree of feature resolution over smooth surfaces. As a result of the polymerisation process used for green body formation, sintering can cause premature crack formation of the part due to polymerisation [101]. Tang et al. [37] describes the use of DLP in the manufacture of highly complex TPMS core structures with a dimensional accuracy of 20 mm³, with fabricated test specimens reported to present uniform grain dispersion, clear crystal arrangement and smooth microstructural surface characteristics. In this case, the UV light had an intensity of 555 $\mu\text{W cm}^{-2}$, wavelength of 405 nm, and a radiation intensity of 72 mW m². Another study by Tang et al. [86] reports on the fabrication of composite precursors for Liquid Silicon Infiltration (LSI) of molten Si to fabricate D_p/SiC and C_f/SiC sandwich structures. The UV light for this investigation had an intensity of 28 mW cm⁻², wavelength of 405 nm, and a radiation intensity of 72 mW m². Both studies immersed the green test specimens in an ultrasonic cleaning machine filled with anhydrous ethanol for 2 min after printing.

Direct Ink Writing (DIW) is a two-stage AM method of water-based extrusion using a viscoelastic ink mixed from a gelatinous ceramic slurry. Prior to manufacture, the ceramic powder must be processed into a gel-based filament that aqueously suspends the ceramic in the viscoelastic ink. The ink possesses shear-thinning behaviour as its viscosity decreases under shear strain, preventing it from deforming after extrusion. Printed layers rapidly solidify due to evaporation, allowing layered extrusion [102]. Sesso et al. [59] and Kim et al. [103,104] explore the manufacture of ZrB₂ CLSSs using DIW with hand-mixed viscoelastic inks incorporating capillary suspension. A primary issue faced by studies

involving the DIW process relates to printing shape retention and sintering shrinkage, both of which are the result of discrepancies in the rheological behaviour of the ink pastes.

3.2.2. Densification

The infiltration processes used in the prototypical fabrication of cellular CMC sandwich structures are detailed in Fig. 8. The most common matrix infiltration technique utilised in the literature is cyclical Polymer Infiltration and Pyrolysis (PIP). PIP is the preform infiltration of a preceramic organo-metallic polymer, predominantly polycarbosilane or polysilane for SiC matrices, which converts into a crystalline or amorphous ceramic via pyrolysis [105]. Successive pyrolysis cycles are required to achieve a suitably dense SiC matrix and the reduction in volume between the precursor and matrix leaves a significant amount of pores, a process that takes place over the course of a few hours depending on the desired number of pyrolysis cycles [83] (Fig. 8). Song et al. [95] achieves an SiC matrix volume of 54 % with a cellular core relative density of 0.176 in test specimens subjected to 9–12 PIP cycles at 1200 °C under 99.99 % pure Nitrogen (N₂). This study does report the identification of micro-defects on the core struts, resulting in the presence of anomalies between the analytical and experiment results.

However, it can be estimated that the defects are a function of the stitching method and strut size used to fabricate the C_f preform, as the same infiltration procedure was incorporated by Yang et al. [96] for the manufacture of trapezoidal sandwich structures without the presence of influential material defects, aside from residual matrix cracks due to

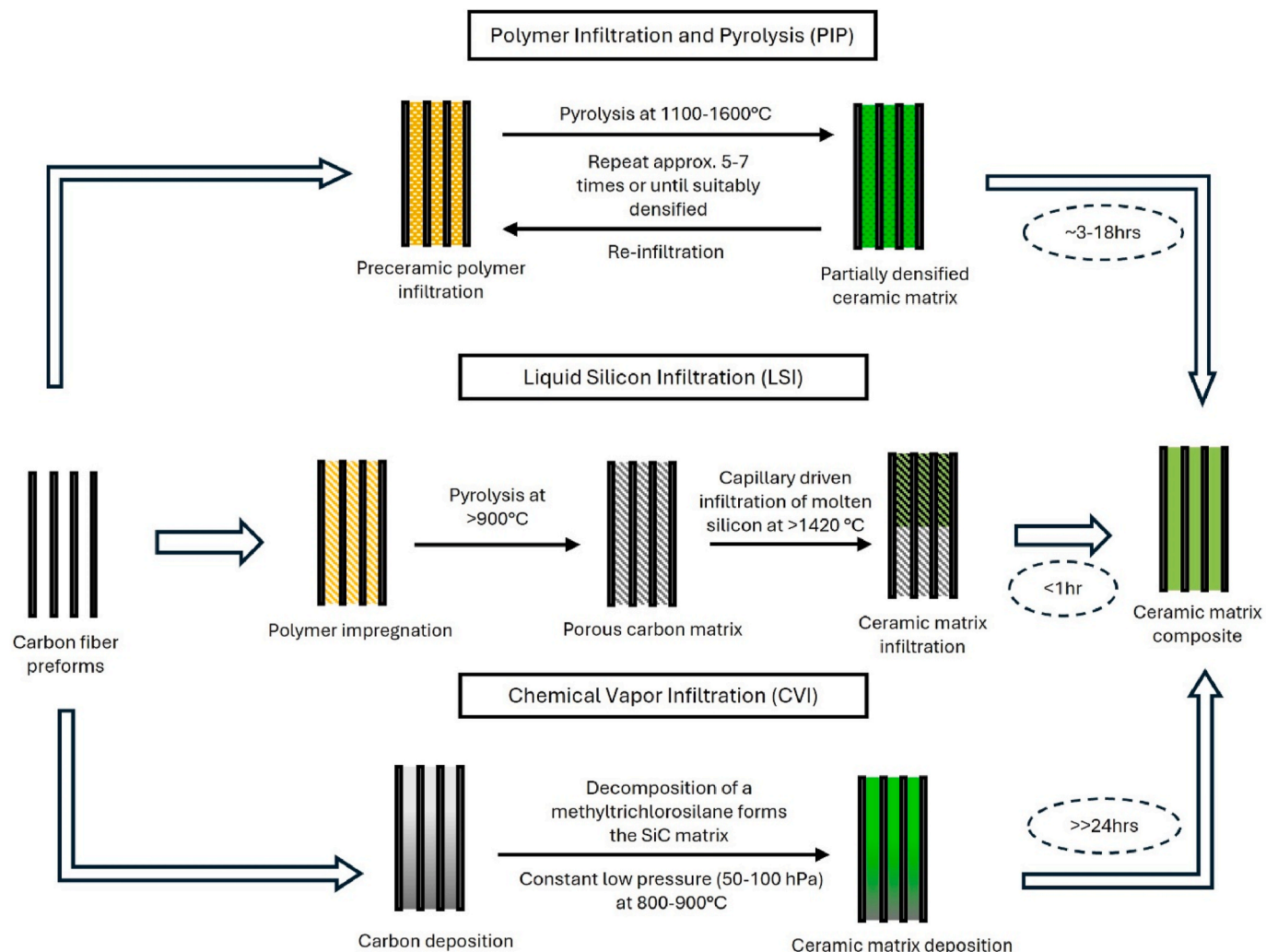


Fig. 8. Matrix infiltration processes for SiC-based CMCs.

pyrolysis shrinkage. Pyrolysis shrinkage is a phenomenon describing the formation of cracks over the surface of a material matrix caused by the abrupt reduction in material volume resulting from the thermo-mechanical decomposition of the preceramic polymer [23,106]. The effects of PIP defects on C_f/SiC sandwich structure performance is explored by Chen et al. [97] who uses microstructural characterisation such as Scanning Electron Microscopy (SEM) to highlight residual defects and crack propagation after PIP cycling. These imperfections have a pronounced impact on the compressive strength of the structures.

In an attempt to improve the mechanical properties of C_f/SiC cellular sandwich structures densified using PIP, Yang et al. [107] investigated the influence of high temperature annealing on the structures compressive strength. Heat treatment of the as-fabricated specimens at temperatures of 1400 °C–1800 °C led to a 3.56 % increase in porosity and a 0.02 g cm⁻³ reduction in relative density. The strength of the C_f/SiC structures are found to increase by approximately 17.4 % after annealing at 1400 °C with quasi-ductile mechanical behaviour observed in both untreated specimens, as expected [23], and those annealing 1400 °C and 1600 °C. Heat treatment at 1800 °C led to 39 % decrease in apparent mechanical strength of the sandwich structures and transformed their failure behavior to brittle [107]. Although this could be a promising avenue for improving the properties of C_f/SiC sandwich structures after fabrication, the risk of creating brittle structures may prove detrimental to high performance structural applications.

Liquid Silicon Infiltration (LSI) is the infiltration of porous C_f/C preforms by molten silicon which siliconizes to form a high density SiC matrix, a relatively fast process which can take less than an hour depending on the size of the preform [23]. Heidenreich et al. [88] employs LSI to densify and bond C_f/C preforms, with infiltration being conducted at a maximum temperature of 1650 °C for 1.5 h. Although time efficient, a few of the test specimens reportedly saw a decline in mechanical strength as a result of excessive C conversion to SiC [88]. Tang et al. [86] investigates the fabrication of composite precursors for an LSI process aimed at the manufacture of D_p/SiC and C_f/SiC sandwich structures with highly complex lattice-core topology. After the green parts were decomposed over a period of 25 h at 600 °C in an Argon atmosphere, LSI was performed in two vacuum heating stages. Initially, the parts were heated to 1900 °C at a rate of 5 °C·min⁻¹ and held for 3 h. The temperature was then reduced to 1000 °C at a rate of 3 °C·min⁻¹ before being cooled to room temperature.

Chemical Vapor Infiltration (CVI) is the deposition of a ceramic matrix over complex, highly porous, but shallow, preforms through the decomposition of gaseous species within the pores. The SiC matrix is formed by the reaction between the process gas, commonly methyltrichlorosilane (CH₃SiCl₃), and a hydrogen catalyst [83]. Whilst CVI produces parts with very good thermo-mechanical properties and improves the fracture toughness of the matrix, the depth of infiltration is very shallow and the process can take upwards of weeks or months depending on the dimensions of the preforms [83]. Wei et al. [94] used this variation of the CVI process at 1100 °C and 5 kPa over an pyramidal sandwich preform, resulting in high quality C_f/SiC test specimens with a uniform matrix distribution. The infiltration time of the CVI process outlined by Wei et al. [94] took a total of 360 h, however the high fidelity of the test specimens streamlined the variation of smaller structural dimensions in the core for extended parametric testing. The use of CVI is also discussed by Hurwitz [77] as being advantageous to the integral densification of C_f/SiC panels with SiC foam cores to avoid the creation of an interface bond layer.

The pressure-assisted HP sintering process employed by Wei et al. [57] to densify a UHTC composite in a single stage. The ZrB₂-20 vol% SiC-15 vol% graphite flake powder was uniaxially hot-pressed in a Boron Nitride coated graphite die at 1900 °C for 60 min at 30 MPa. The geometrical constraints of pressure-assisted sintering processes can be observed in the lack of net shape formation, as electrospark wire-electrode cutting was required to cut out the corrugate core topology from the densified ZSG solid [57]. Alternative studies by Wei

et al. [85] and Sesso et al. [59] discuss the use of pressureless sintering for part densification. The ZrO₂ corrugated structures fabricated by Wei et al. [85] were densified via pressureless sintering at a temperature of 1450 °C. Sesso et al. [59] utilised a graphite vacuum furnace to densify 3D printed ZrB₂ following a two stage pressureless sintering procedure. Debinding was conducted by vacuum heating of the test specimens at a rate of 5 °C·min⁻¹ from room temperature to 400 °C, from at which point the temperature was isothermally held for 60 min. The samples were then heated to maximum temperatures of either 1800 °C or 2000 °C at a rate of 10 °C·min⁻¹ before being held for 60 min of isothermal heating. The densified ZrB₂ structures were then cooled to room temperature at a rate of 10 °C·min⁻¹. The inadequacy of pressureless sintering for the densification of UHTCs is observed experimentally by Sesso et al. [59] as densified test bars presented an average bulk density of 29.2 % with resultant porosities of each specimen falling within the range of ~70–80 %.

Select Laser Sintering (SLS) is a powder bed fusion AM process that utilises a high intensity Carbon Dioxide (CO₂) laser to sinter specified preheated layers of a powdered ceramic to form a given geometry. The direct densification capability of the high intensity laser streamlines AM process whilst maintaining high part fidelity [99]. Mei et al. [100] reports the accuracy afforded by SLS which allows the manufacture of Body Centred Cubic (BCC) lattice core test specimens using modified SiC powders and photosensitive resin with complex, multilayered BCC core topologies. Following SLS fabrication of the SiC structures, the core architecture is filled with quartz fibers possessing a volume density of 0.25 g cm⁻³ with a diameter of 3–5 μm to create an internal fiber preform for the integration of a Quartz fiber reinforced Silica (Q_f/SiO₂) aerogel insulation layer. The SiO₂ aerogel was manufactured using the sol-gel method, a process involving the hydrolysis and condensation of a silicon precursor to create a sol. The sol is then used impregnate fibrous preforms to create an aerogel, which in this case was the quartz fiber preforms dispersed through the lattice core of the SiC sandwich structure. The Q_f/SiO₂ aerogel insulation was solidified through CO₂ supercritical drying, and the successful dispersion of the composite was confirmed by the wormlike structure observed through micromorphological analysis [100]. Li et al. [68] also describes the use of both internal and external aerogel layers to improve the insulative performance of a C_f/SiC corrugated core sandwich structure, however the aerogel material composition as well as the method of manufacture and integration into the existing cellular sandwich structure are not reported. A summary of the advantages and disadvantages of key forming and densification procedures is provided in Table 3.

The replication method outlined in Fig. 9 is proposed by Ortona et al. [93,108] for the fabrication of complex, Si-based ceramic structures through the infiltration of Si onto a complex polymer part manufactured using photopolymeric AM. The three-step process involves the impregnation of an additively manufactured photopolymer structure with an Si-based ceramic slurry. The coated structure is dried and subjected to pyrolysis which decomposes the photopolymer substrate, leaving behind residual carbon that reacts to form additional SiC via LSI. Substrate decomposition under the ceramic facilitates its replication as a lightweight ceramic structure with hollow core trusses. The hollow trusses of replicated structures do not suffer excessive mechanical strength losses, conversely exhibiting compressive strength enhancements as reported by Ortona et al. [108] due to the lack of internal stress concentrations. Ferrari et al. [67] used the replication method to create complex hexahedral cuboid lattice-cores for a leading edge actively cooled Silicon-Infiltrated Silicon Carbide (SiSiC) sandwich structure. The resulting test specimens were of high quality with no discernible manufacturing related damage. Although being an accurate and effective SiC fabrication method, currently replication is only compatible with Si-based ceramic fabrication techniques.

3.2.3. Bonding mechanisms

Bonding mechanisms between the porous core and dense face sheets

Table 3

Characteristics of different ceramic manufacturing methods investigated for the fabrication of ceramic sandwich structures.

Process	Studied Materials	Advantages	Disadvantages	Refs.
Chemical Vapor Infiltration (CVI)	C_f/SiC	<ul style="list-style-type: none"> Control over the fiber/matrix interphase Low infiltration temperatures prevent carbon fiber damage High matrix purity 	<ul style="list-style-type: none"> Long infiltration times (>24hrs) Gas cannot reliably penetrate deep preforms 	[83,94]
Polymer Infiltration and Pyrolysis (PIP)	C_f/SiC	<ul style="list-style-type: none"> Control over matrix composition and porosity Low polymer to ceramic conversion temperatures prevents matrix fiber damage 	<ul style="list-style-type: none"> Polymerisation shrinkage during pyrolysis can lead to crack generation Production times for parts requiring many PIP cycles can be very long 	[23,95]
Liquid Silicon Infiltration (LSI)	C_f/SiC , $\text{C}-\text{C}_f/\text{SiC}$	<ul style="list-style-type: none"> Fast matrix infiltration (<1hr) Low shrinkage High quality material joints 	<ul style="list-style-type: none"> Molten Si can damage C fibres Residual Si can remain in the matrix 	[23,88]
Gel-casting	ZrO_2	<ul style="list-style-type: none"> Compatible with large part sizes Well documented processes 	<ul style="list-style-type: none"> Poor part fidelity Limited allowable part complexity 	[85,98]
Uniaxial Hot Pressing	ZrB_2 , ZSG	<ul style="list-style-type: none"> Combined forming/sintering process reduces production time Can sinter ceramics with very high melting points 	<ul style="list-style-type: none"> Limited allowable part complexity Requires additional finishing procedure to cut out sandwich core 	[57,80,89]
Select Laser Sintering (SLS)	SiC_p/SiC , SiC	<ul style="list-style-type: none"> Single-step process reduces manufacture time Minimal waste 	<ul style="list-style-type: none"> High material waste Poor surface finish Low part resolution 	[25,99]
Direct Ink Writing (DIW)	ZrB_2	<ul style="list-style-type: none"> Rapid room temperature solidification Can capture very fine part details Can fabricate very complex designs 	<ul style="list-style-type: none"> High melting point ceramics require slurry dilution Reliant on viscoelasticity of ink Ink additives may cause part defects 	[59,102]
Digital Light Processing (DLP)	SiC	<ul style="list-style-type: none"> High feature resolution Fast production time Minimal waste 	<ul style="list-style-type: none"> Risk of volumetric shrinkage and crack formation Polymerisation shrinkage can lead to cracks in the green body 	[37,101]
Replication	SiC , SiSiC	<ul style="list-style-type: none"> Hollow core struts provide significant weight reductions As accurate and complex as the photopolymer template Low shrinkage and crack density 	<ul style="list-style-type: none"> Lengthy, multi-stage production process Residual polymeric binders may become trapped in material 	[67,108]

are important in determining the effective bending strength, damage tolerance, and thermal shock resistance of the overall structure as the interface joints between the sandwich components are inherent weak points in the structures design. A key advantage to the use of monolithic ceramics is associated with their intrinsic net shape manufacturing processes that avoid the need for core to panel bonding [37]. Although the joint location between the core and face sheets remains a topological weak point [85], the risk of bond shear failure during bending is eliminated and localised thermal shock resistance is improved as a result of structural homogeneity [93]. However, the presence of a bond layer is difficult to avoid in the design of CMC sandwich structures due to the net shape limitations of fibrous preform fabrication with respect to enclosed structures and architectural cellular networks. Various methods of structural bonding have therefore been reported in an effort to minimise bond layers impact on the thermomechanical response of cellular CMC sandwich structures.

The application of commercial joining pastes and adhesives streamlines the preforming process as reported by Heidenreich et al. [88] in the joining of C_f/C preforms. A carbon-based, commercial joining paste was applied to a steel plate with a constant 3 mm thickness. The core structure was then dipped into the paste layer and placed onto a single face where the paste is subsequently cured at a temperature of 220 °C for 4 h prior to siliconization. Inducing crosslinking solidification between face sheet and core preforms is a common strategy of joining sandwich components prior to densification. Yang et al. [96] and Song et al. [95] utilise an autoclave to promote crosslinking solidification of a trapezoidal unit cell fit into a steel mould, whereas Chen et al. [97] reports the use of a vacuum pressure immersion machine. In all cases described in the literature, crosslinking of the preforms is achieved using identical parameters with a constant pressure of 0.3 MPa and heated to 120 °C for 180 min and then 150 °C for 180 min. By interweaving C_f bundles between the face sheets for pyramidal unit cell preforming, Wei et al. [94] avoids the need for a bonding layer within the sandwich structure core interface.

Bonding of SiC foam cores to CMC panels is considerably more intricate in comparison to structured cellular networks due to the

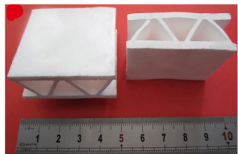
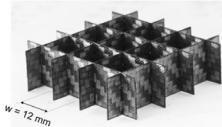
irregularity, size, and number of contact points constituting the core interface. NASA developed a method of allowing the integral densification of C_f/SiC panels to SiC foams via CVI without bond layer adhesion as reported by Hurwitz [77]. To achieve this, the CTE of both sandwich components was matched via tailoring of their material compositions such that they can be interwoven without risk of delamination during matrix infiltration. An *in-situ* method for the joining of an SiC foam core with C_f/SiC face sheets is developed by Ortona, Pusterla, and Gianella [93] which describes impregnation of the sandwich interface with a polymeric precursor prior to PIP densification, creating a strong bond layer between the embedded core and face sheets. Gianchandani et al. [109,110] presented pressure-less methods of *in-situ* brazing C_f/SiC and SiC/SiC face sheets to $\text{Si}-\text{SiC}$ cores using a composite fabricated by wrapping Molybdenum (MoSi_2) foil around a thin strip of Silicon (Si). The composite is placed between the sandwich components and heated at 1450 °C for 5 min with a heating rate of 1000 °C/h under Argon to form a solid bond in the form of a thin material layer characterised by embedded MoSi_2 particles in a Si matrix. Foam core sandwich structures manufactured using this method are found to exhibit sound compressive strength properties and are able to effectively resist thermal shock at temperatures up to 1100 °C [110].

3.3. Hot ceramic sandwich structures

Hot ceramic sandwich structures are simply designed to operate for extended periods of time within the hypersonic flow regime without additional thermal management, taking full advantage of the superior thermal properties afforded by monolithic ceramics. More than half of reported studies into ceramic sandwich structures can be defined as hot structures, being distinguished primarily by a lack of additional TPS integration. The following sections aim to critically analyse the design strategies and resultant performance parameters of currently reported works categorized by the classification of their core topology. Properties of the sandwich structures, methods of characterization, as well as both qualitative and quantitative findings of significant studies are summarized in Tables 4–7. Methods employed for the experimental, numerical,

Table 4

Major findings of studies into planar sandwich structures.

Year	Topology	Material	Structure	Methods	Major Findings	Refs.
2014, 2017	Corrugated	ZrO ₂		3 PB; UC; FEA; TMT; ATM	<ul style="list-style-type: none"> Relative density of the ZrO₂ structures is only 42.9 % of the bulk ceramic at 2.4 g cm⁻³ Compressive strength measured to be 11.8 MPa@RT and 8.5 MPa@1000 °C The specific bending strength is measured to be 124.3 MPa/(g. cm⁻³)@RT and 124.3 MPa/(g. cm⁻³)@1000 °C. These results are found to be twice as high as the bulk material. The failure mode in both bending and compression is observed to be core sheet fracture. 	[85,89]
2015	Corrugated	ZSG		UC; TMT; HTT; FEA; ATM	<ul style="list-style-type: none"> Relative density of the ZSG structures measured to be 2.0 g cm⁻³, a 59.4 % reduction over the bulk ceramic. Three distinct oxidation layers observed to form at 1600 °C High temperature compressive strength measured to be 17 MPa@1600 °C Core-sheet connections identified as weak points in the structure through FEA simulation. Truss buckling is identified as the primary mode of mechanical failure at ultra-high temperatures. 	[57,117]
2017, 2018, 2020	Grid	C/C-SiC		4 PB; 3 PB; FEA; ATM;	<ul style="list-style-type: none"> The thin strips used to construct the core yield an ultra-low core density of 0.09 g cm⁻³ Overall sandwich structures had relative densities in the range of 0.267–0.275 g cm⁻³ The most common failure mode observed during bending was debonding of the core structure from the outer panels Fiber orientation in the core relative to the load axis played an influential role in dictating the shear resistance and stiffness of the panels Samples with ±45° fiber orientations had superior flexural properties to those with 0°/90° compositions Relative density of the test specimens are measured at 1.1 g cm⁻³, a 47.7 % reduction in density compared to the bulk material Compressive strength of the structure is found to be 15.1 MPa. The mode of failure in compression was a debonding of the corrugated core with the face sheets. The structures have a flexural load capacity of 1947 N before failure through shear failure of the core trusses. 	[88, 114–116]
2021	Corrugated	C _f /SiC		UC; 3 PB; FEA	<ul style="list-style-type: none"> Relative density of the test specimens are measured at 1.1 g cm⁻³, a 47.7 % reduction in density compared to the bulk material Compressive strength of the structure is found to be 15.1 MPa. The mode of failure in compression was a debonding of the corrugated core with the face sheets. The structures have a flexural load capacity of 1947 N before failure through shear failure of the core trusses. 	[97]
2021, 2022, 2023	Honeycomb and Logpile	ZrB ₂		UC; 4 PB; ATM;	<ul style="list-style-type: none"> Test specimens presented relative densities in the range of 4.33–5.68 g cm⁻³ with porosities in the range of 71.5–83.5 % The bending strength of the bars were in the range of 0.97–10.4 MPa A Weibull analysis of the experimental results was used to determine a characteristic strength of 3.58 MPa with a corresponding Weibull modulus of 2.05. Truss fracture in the cores was the primary mode of failure for both topological configurations 	[59,103, 104]

and analytical analysis of the structures are provided within the summaries as acronyms for the following abbreviations: Uniaxial Compression (UC); 3 Point Bending (3 PB); 4 Point Bending (4 PB); Thermomechanical Testing (TMT); Heat Transfer Testing (HTT); Finite Element Analysis (FEA); Computational Fluid Dynamics (CFD); Analytical and Theoretical Modeling (ATM).

3.3.1. Corrugated core

Corrugated core configurations as described in Fig. 10a are a common design choice for sandwich structures that require very high strength-to-weight ratios, a desirable offset to the poorer mechanical properties of conventional ceramics. They have become an established design for hypersonic structures and provide the foundation for a robust optimisation procedure that aims to prioritize internal allowable stress, buckling, and deflection with respect to a minimum total weight [111].

Wei et al. [85] manufactured corrugated core ZrO₂ sandwich structures using a gel-casted and pressure-less sintering process. Initial mechanical characterisation showed significant improvements to the bulk material properties including a 53 % density reduction and a 114 %

increase to the specific bending strength. Thermomechanical testing at the materials service temperature of 1000 °C showed little change in the structure's mechanical properties with respect to temperature [89]. A subsequent study by Wei et al. [57] improved the service temperature of the structure up to a maximum tested temperature of 1600 °C through the use of the ZSG composite. Similarly, the composite sandwich structures also possessed a lower relative density with comparable compressive strength characteristics to its monolithic forerunner.

To improve the strength-to-weight performance of the corrugated core design whilst reducing the amount of thermally conductive material in the core, Yang et al. [96] proposes the use of a corrugated geometry with discontinuous vertical supports. As depicted in Fig. 10b, this creates a three-dimensional trapezoidal unit cell with a noticeably lower material distribution compared to its corrugated precursor (Fig. 10a). C_f/SiC sandwich structures based on this core design are evaluated on their oxidative behaviour with an apparent increase to mechanical strength observed at higher oxidation temperatures between 1200 and 1600 °C, albeit retracing rapidly after extended exposure. The strength of the C_f/SiC structures are found to increase by approximately

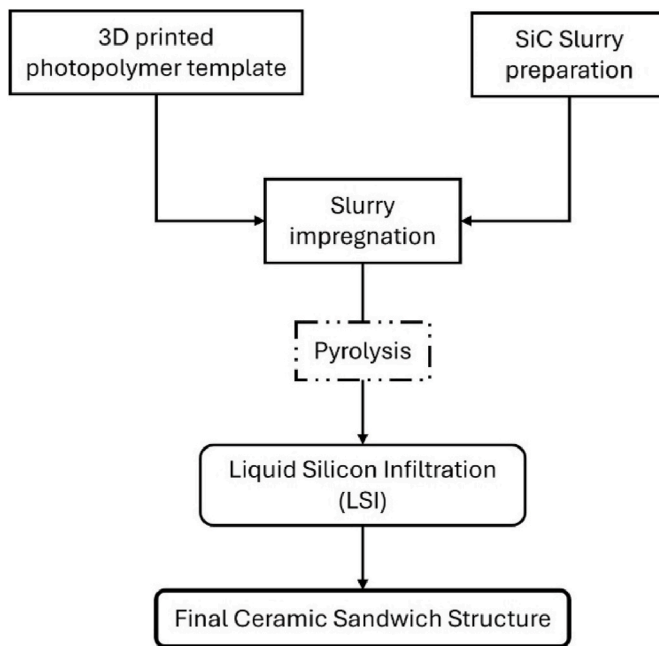


Fig. 9. Replication manufacturing process.

17.4 % after annealing at 1400 °C and displayed ductile behaviour after annealing at both 1400 and 1600 °C, however strength reductions are observed after a similar process is conducted at 1800 °C [107].

The influence of corrugated trapezoidal truss inclination angle on the in- and out-of-plane mechanical response of C_f/SiC sandwich structures was investigated by Zhang et al. [106]. A truss angle of 30° is observed to correlate with the highest measured bending strength, although a core angle of 75° is found preferential for out-of-plane compression loading. A common trend in failure mode transition emerged during testing for cores with higher inclination angles. They were reported to fail due to interlayer delamination compared to core buckling or crushing, a phenomenon inherent to the embedded fibre composition of CMCs. The subsequent development of numerical models by Zhang et al. [112] simulates the bending response and failure behaviour of the C_f/SiC composites using the elastic-constitutive model. The cohesive crack approach was used to simulate interlayer delamination, displaying a very close approximation of the experimental results.

Chen et al. [38] developed an analytical and numerical design methodology that minimizes risk of delamination in C_f/SiC trapezoidal sandwich structures through failure mapping. The maps are found to show very good agreement with the results of corresponding FEA models. Relationships between inclination angle, face sheet thickness, and compressive strength are quantified and used to optimize structures that exhibit face sheet crushing failure regardless of inclination angle. These strategies provide a promising method of optimizing the failure modes of ceramic sandwich structures and avoiding delamination in CMCs, but fail to compensate for material imperfections which can lead to unpredictable intra-face delamination [38].

The specific thermal insulation performance of a trapezoidal C_f/SiC sandwich structure up to a maximum temperature of 1200 °C is investigated by Chen et al. [113], a boundary condition that remains conservative for hypersonic applications. A robust analytical model is developed to compensate for the effects of external surface radiation, providing a method for the design and numerical analysis of different sandwich structure configurations aiming to minimise the effects of cavity radiation [36]. Creating multiple core layers separated by Middle Face Sheets (MFSs), as detailed in Fig. 11a, is an effective method of significantly reducing the severity of cavity radiation without integrating additional internal insulation. Sandwich structures comprised of

two, three, and four layers were numerically modelled to determine their effective thermal conductivity as a function of temperature. As expected, the addition of a second layer reduced the effective thermal conductivity of the sandwich structure by approximately half under a thermal load of 1200 °C. Interestingly, additional layers up to a maximum of four (Fig. 10b) led to increases in the overall effective thermal conductivity of the taller structures [113].

Overall, the effectiveness of corrugated core topologies is limited by the simple core architecture which leaves little room for design stage optimisation. The open nature of the core works against the insulation function of the structure, with reports indicating that cavity radiation becomes the dominant mechanism of heat transfer at low temperatures [89,113].

3.3.2. Honeycomb cores

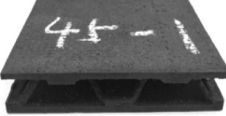
Honeycomb core designs are another longstanding sandwich structure configuration in the field of aerospace design due to their desirable strength-to-weight and energy absorption characteristics. A summary of major findings into key experimental studies of both corrugated and honeycomb planar core sandwich structures is provided in Table 4. Sesso et al. [59] reports on the design and mechanical characterisation of novel ZrB₂ honeycomb (Fig. 12a) and open-cell cubic core sandwich structures additively manufactured using DIW. A combination of SEM, X-ray tomography and four-point bending analysis are used to characterise the structural characteristics of the sandwich structures, the results of which reach parity with comparable strength-to-density ratios reported by alternative studies into the AM of technical oxide ceramics. The empirically determined properties form the basis for development of an analytical model that can predict the elastic moduli of the sandwich structure for a given print architecture and core porosity. Kim et al. [103,104] provides a more comprehensive review of the 3D printed ZrB₂ honeycomb and cubic sandwich structures, including an additional microstructural analysis of the core topology before and during four-point flexural analysis. X-ray Computed Microtomography (μXCT) allows observation of prominent imperfections that transform into cracks under flexural loading. A well-defined relationship between higher relative density and improved structural performance is also observed within both configurations.

A vertically oriented cubic honeycomb configuration, known as a grid core (Fig. 12b), is proposed by Heidenreich et al. [88] alongside a folded core topology for the construction of C_f/C-SiC sandwich structures with enhanced flexural and stiffness properties. Three-point bending analysis reported that whilst folded core specimens all exhibited brittle skin fracture, the grid core configurations predominantly failed through core debonding between the face sheets and shear fracture of the internal supports. Compared to a solid plate, the effective flexural strength of folded and grid core C_f/C-SiC sandwich structures were found to be 54 times higher and required a bending magnitude up to 7 times larger before fracture. However, these performance increases are less impressive relative to alternate CMC sandwich structure designs and the shear strength of grid cores was lower relative to folded configurations. The initial investigation by Heidenreich et al. [88] represents one of the few, if not the only, descriptions of folded core configurations in the design of hypersonic ceramic sandwich structures.

Follow up studies by Shi et al. [114,115] and Heidenreich et al. [116] consolidate their focus towards grid core C_f/C-SiC sandwich configurations, with the former providing a comprehensive approach to the characterisation of bending properties using a combination of analytical, numerical, and experimental methods. Fibre orientation in the core material is found through four point bending analysis to significantly influence structural stiffness, allowing determination of the optimal orientation at 0/90° ± 45° using the combined modelling approach. It is also reported that the contribution of the core architecture to the overall effective stiffness of the sandwich structure only becomes significant at larger core heights. Heidenreich et al. [116] demonstrated the scalability of the near net shape fabrication process and incorporated both

Table 5

Major findings of studies into periodic and array-based lattice core sandwich structures.

Year	Topology	Material	Structure	Methods	Major Findings	Refs.
2014, 2015, 2017	Pyramidal	C _f /SiC		FEA; ATM; HTT; TMT	<ul style="list-style-type: none"> Relative density of the structure is only 5.18 % of the bulk density In the temperature range from 600 to 1150 °C, the effective thermal conductivity of the structure increases from 1.98 to 4.95 W m⁻¹ K⁻¹ Insulation efficiency is measured at 90 % during transient heat transfer testing, but settles to value of 20 % once thermal equilibrium is reached Cavity radiation is shown through FEA modeling to be the primary motivator of reduced thermal performance at high temperatures The compressive strengths of the structure is measured to be 12.70 MPa@RT, 5.35 MPa@1200 °C, 2.45 MPa@1600 °C The primary mode of failure in compression was strut fracture The specific bending strength is measured to be 260.7 MPa/(g.cm⁻³)@RT, 168.7 MPa/(g.cm⁻³)@1200 °C, and 152.1 MPa/(g.cm⁻³)@1600 °C Shear failure of the core struts are the primary mode of failure in bending 	[94,118, 120]
2015	Pyramidal	C _f /SiC		UC; ATM	<ul style="list-style-type: none"> The out-of-plane compressive strength of the panel is measured to be 20.97 MPa. In-plane compressive strength was found to be 165.61 MPa at its peak The primary mode of failure was observed to be debonding and fracture of the stitched yarns used for core construction Micro-defects in the stitching led to data discrepancies between the experimental and analytical results for compressive strength 	[95]
2016, 2019, 2020, 2021	Trapezoidal	C _f /SiC		UC; TMT; ATM; FEA;	<ul style="list-style-type: none"> Relative density of test specimens was measured in the range of 1.88–2 g cm⁻³ with an approximate porosity of 20 % after 8 PIP cycles The compressive strength of the panels is measured at 2.69 MPa@RT The strength of the structure decreased by 25 % after 30 min of exposure to oxidation at temperatures of 1200 °C but improved to a 12 % drop when the temperature was increased to 1600 °C After 90 min of exposure to 1600 °C oxidation, the structures strength was reduced by approximately 33 % Oxidation was observed to transition the failure mode of the C/SiC structures from quasi-ductile to brittle fracture Unexpected interlayer delamination as a result of specimen imperfections is observed during buckling experimentation At inclination angles of 30°, 45°, 60°, and 75° the specific bending strengths are found to be 24.76, 21.97, 17.78, and 11.29 MPa/(g.cm⁻³), respectively. Similarly, out-of-plane compressive is found to be 0.37, 0.67, 0.86, and 1.18 MPa/(g.cm⁻³) for each respective inclination angle. The failure mode transitioned from strut buckling to interlayer delamination at higher inclination angles 	[38,96, 106,107, 112,113]
2020	Pyramidal	SiC _p /SiC		UC; TMT; ATM	<ul style="list-style-type: none"> Relative density of the structure increased by a factor of 2.1 after PIP from 1.3 to 2.67 g cm⁻³ Compressive strength is found to increase in proportion to higher inclination angles. At 60°, the compressive strength is 45.66 MPa. Increasing the temperature of the structure from 1400 °C to 1800 °C resulted in a 34.3 % decrease in compressive strength. The mechanical behaviour of the structure became non-linear at a temperature of 1800 °C 	[82]
2024	TPMS: Gyroid	SiC		FEA; ATM; HTT	<ul style="list-style-type: none"> Low effective thermal conductivities are found to correspond to higher lattice porosity At 40 % porosity, the effective thermal conductivity is determined to be 4.3 W m⁻¹ K⁻¹, nearly half that of the bulk conductivity of 8 W m⁻¹ K⁻¹ The average emissivity of the lattice was measured at 0.95 on a 1.28–25 μm wavelength scale, being considerably higher than bulk SiC which exhibited an emissivity of 0.85 over a similar scale 	[37]

(continued on next page)

Table 5 (continued)

Year	Topology	Material	Structure	Methods	Major Findings	Refs.
2024	TPMS: Diamond, Gyroid, IWP	D _p /SiC; C _f /SiC		FEA; UC; HTT; ATM	<ul style="list-style-type: none"> D_p/SiC remained mechanically unaffected at 800 °C compared to a near 50 % drop in the yield strength of C_f/SiC The 45° angular struts of the diamond TPMS lattice exhibits greater yield strength in comparison to Gyroid and IWP core topologies The average thermal conductivity of D_p/SiC is 6.5 W m⁻¹ K⁻¹ compared to the measured 5.6 W m⁻¹ K⁻¹ of C_f/SiC 	[86]

Table 6

Major findings of studies into foam lattice sandwich structures.

Year	Topology	Material	Structure	Methods	Major Findings	Refs.
2009	Foam	C _f /SiC (face); SiC (core)		HTT	<ul style="list-style-type: none"> CTE of the core and face sheets are matched by tailoring the constituent composition, allowing integral densification and eliminating core to face sheet bonding The relative density of the final structure is 1.06 g cm⁻³. Capable of withstanding heat fluxes up to 150 W cm⁻² with a temperature differential of 1000 °C between each face sheet without signs of thermal shock damage 	[77]
2011	Foam	C _f -SiC _f /SiC (face); SiC (core)		3 PB	<ul style="list-style-type: none"> The integration of a SiC foam core prevent catastrophic failure of the structure Sandwich structures exhibit flexural strengths approximately 6 times higher than a plain foam with a flexural strength of 2.64 MPa Skin thickness is not found to influence flexural strength 	[93]
2017, 2018	Foam	C _f /SiC (face); SiC (core)		UC; TMT	<ul style="list-style-type: none"> Joining foam SiC cores with C_f/SiC face sheets is accomplished using a MoSi₂/Si composite joining material to avoid the infiltration of molten Si into the foam structures. The joints can withstand a compressive load up to 710 N, which is comparable to the as-fabricated SiC foam at 700 N. The core to face sheet joints successfully withstood thermal shock up to a temperature of 1100 °C 	[109, 110]

three and four-point bending tests to quantify the properties of grid core C_f/C-SiC sandwich structures with various fibre orientations. Building on prior work, total effective stiffness was observed to increase by 45–59 % through reorientation of the core fibres 0/90° ± 45° without altering the system weight. As is evident, the scope of reported work into the development of grid core sandwich structures is narrow and lacks characterisation of their thermal performance which hinders their applicability to high temperature applications.

3.3.3. Lattice core

Lattice cores represent a complex class of cellular architecture that provide an unparalleled degree of strength-to-weight, energy absorption, and thermal performance that make them ideal candidates for hypersonic design. Whilst they constitute a substantial portion of the current research studies into the design of ceramic sandwich structures, the complexity limitations associated with CMC manufacture have stifled the diversity of studied topologies. Reported works therefore rely on the superior structural properties of CMCs and defer the core design to arrays of simple, asymmetric pyramidal unit cells, as detailed in Fig. 13a, are asymmetric with only two degrees of periodicity but simple enough to be manufacturable with matrix composites. At present, only a handful of alternative unit cells with full periodicity have been reported for use in ceramic hot structures including Triply Periodic Minimal Surface (TPMS) Schoen-gyroid (Fig. 13b) and open-cell cubic (Fig. 13c), both of which generally require some method of AM for fabrication. A summary of key findings from prominent experimental studies into periodic and array-based lattice core sandwich structures is provided in Table 5.

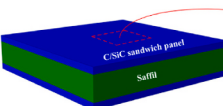
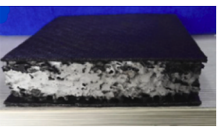
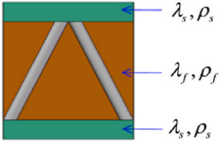
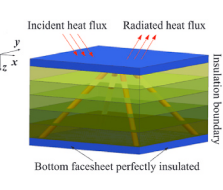
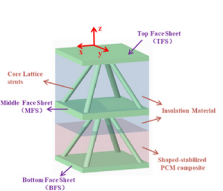
Initial research into lattice core ceramic sandwich structures began in response to the need for lightweight load bearing insulators for

aerospace applications. Coupled with a lack of study into the heat transfer characteristics of C_f/SiC, Wei et al. [94] launched an investigation into the high temperature performance of pyramidal C_f/SiC sandwich structures. Three point bending tests highlighted a high retention rate of flexural strength alongside a 95 % reduction in relative density compared to the bulk material properties. Preliminary heat transfer analysis through numerical modelling identified the presence of cavity radiation during 1000 °C loading, resulting in poorer insulative performance as determined by the adverse emissivity of the core architecture. Reducing the internal truss length was found to be an effective method of altering core emissivity at the cost of mechanical strength.

The relationship between truss length and the effective material properties formed the basis of a proposed design reference and methodology developed by Wei et al. [118]. This strategy aimed to balance the insulative properties, stiffness, and yield failure surfaces of the structure. At a maximum thermal load of 1150 °C, the insulation efficiency of the structure (determined as the ratio of TFS to BFS surface temperature) was reduced from a transient peak of 90 % to a steady-state 20 % over the course of 150 s. The dominance of cavity radiation during high temperature loading is partially attributed to the temperature dependence of the materials bulk thermal conductivity as it experienced a 2.5x increase from 600 to 1150 °C. During maximum load conditions, the test specimens endured minor face sheet warping and debonding whilst the core trusses experienced premature ablation. The observations of this investigation led to the construction of an analytical model that is able to predict the effective thermal conductivity of a lattice core sandwich structure by considering both conductive and radiative heat transfer by Cheng et al. [36]. The integration of additional core material, multilayering the core configuration, and optimizing the

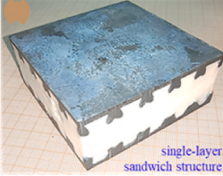
Table 7

Major findings of studies into cellular ceramic sandwich structures with integral TPS.

Year	Topology	Structural Material	Ins. Material/Coolant	Structure	Methods	Major Findings	Refs.
2016	Internally Insulated Pyramidal	$\text{C}_\text{f}/\text{SiC}$	$(\text{Al}_3\text{O}_2)_\text{f}$		FEA; ATM	<ul style="list-style-type: none"> Effective thermal conductivity is reached from the temperature dependent range of $2.45\text{--}4.83 \text{ W m}^{-1} \text{ }^\circ\text{C}^{-1}$ to a theoretically consistent $0.7 \text{ W m}^{-1} \text{ }^\circ\text{C}^{-1}$ with the addition of $(\text{Al}_3\text{O}_2)_\text{f}$ The critical relative density is identified to ensure the failure model of the insulated structure is core strut fracture, a failure mode that is no longer catastrophic with a dense composite core At $200 \text{ }^\circ\text{C}$ and $180 \text{ }^\circ\text{C}$, the areal density of the insulated structure is 0.0391 g cm^{-2} and 0.0436 g cm^{-2}, respectively 	[135]
2017	Internally Insulated Foam	$\text{C}_\text{f}/\text{SiC}$	SiO_2 powder		HTT; ATM	<ul style="list-style-type: none"> Relative density of the compound SiC core is 1.31 g cm^{-3} The effective thermal conductivity of the core is measured in the range of $0.529 \text{ W m}^{-1} \text{ }^\circ\text{C}^{-1}$ @ $100 \text{ }^\circ\text{C}$ to $0.603 \text{ W m}^{-1} \text{ }^\circ\text{C}^{-1}$ @ $900 \text{ }^\circ\text{C}$. In comparison, the bulk $\text{C}_\text{f}/\text{SiC}$ panels have thermal conductivities in the range of $7.24 \text{ W m}^{-1} \text{ }^\circ\text{C}^{-1}$ @ $100 \text{ }^\circ\text{C}$ to $2.91 \text{ W m}^{-1} \text{ }^\circ\text{C}^{-1}$ @ $900 \text{ }^\circ\text{C}$ 	[128]
2018	Internally Insulated Pyramidal, Corrugate, Trapezoidal	$\text{C}_\text{f}/\text{SiC}$	Glass wool		FEA; ATM	<ul style="list-style-type: none"> The effective thermal conductivity is a direct function of core height, with larger core spans providing more internal insulation and thus reduced heat transfer Pyramidal core topologies provide a much higher insulative potential compared to corrugate or trapezoidal structures Comparisons with Ti and Beryllium alloy insulated sandwich structures in the literature highlight an approximate 50 % reduction in areal density and 400–900 °C improvement to the structures service temperature 	[125]
2019	Internal and externally insulated Corrugate	$\text{C}_\text{f}/\text{SiC}$	Generic aerogel		FEA; HTT; ATM	<ul style="list-style-type: none"> Under a thermal load of $1400 \text{ }^\circ\text{C}$, the internally insulated structure was reported to maintain a consistent BFS temperature of $\sim 700 \text{ }^\circ\text{C}$ This was a $\sim 500 \text{ }^\circ\text{C}$ reduction compared to an uninsulated sandwich structure configuration The addition of a 12 mm layer of aerogel to the BFS of the insulated structure was observed during experimental re-entry testing to reach a maximum temperature of $220 \text{ }^\circ\text{C}$ 	[68]
2019	Functional gradient insulated pyramidal, corrugate	$\text{C}_\text{f}/\text{SiC}$	$(\text{ZrO}_2)_\text{f}$; (Mullite) $_\text{f}$; $(\text{Al}_3\text{O}_2)_\text{f}$; $(\text{Al}_2\text{SiO}_5)_\text{f}$; Glass wool		FEA; ATM	<ul style="list-style-type: none"> Grading insulative layers in a hierarchy based on the lowest thermal conductivity and density offers a higher degree of thermal efficiency than an inversely graded arrangement. Under a heat flux of 50 kW m^{-2} the pyramidal structure is reported to maintain a steady state BFS temperature of $130 \text{ }^\circ\text{C}$ whilst the corrugate structure presents a temperature of $220 \text{ }^\circ\text{C}$ Alongside suppression of cavity radiation and improved thermal performance, the addition of graded insulation layers also improves the buckling strength of the core topology 	[130]
2023	Phase change composite insulated pyramidal	$\text{C}_\text{f}/\text{SiC}$	Generic aerogel with fibre insulation; 90 wt % paraffin/10 wt% expanded graphite composite PCM		FEA; ATM	<ul style="list-style-type: none"> The addition of a second array layer in the bilayer configuration is demonstrated to greatly reduce the effects of thermal short circuiting, improving PCM heat absorption Aerogel with fibrous insulation provides higher thermal performance than standard aerogel A 10 mm layer of a PCM composition designed with a thermal conductivity of $0.82 \text{ W m}^{-1} \text{ K}^{-1}$ is found to provide the 	[123]

(continued on next page)

Table 7 (continued)

Year	Topology	Structural Material	Ins. Material/Coolant	Structure	Methods	Major Findings	Refs.
2023	Internally insulated BCC	SiC	Q _f /SiO ₂ aerogel		FEA; ATM; UC; HTT	<p>best insulative performance with a maximum BFS temperature of 43.24 °C</p> <ul style="list-style-type: none"> Reducing the diameter of the core struts by 0.5 mm improves the thermal performance of the structure through a 13.12 °C temperature reduction of the BFS, at the cost of reduced mechanical strength The optimal internal insulation composition consists of a 10 mm PCM layered under 20 mm of aerogel insulation fibre and a strut diameter of 1.5 mm. Under a thermal load of 2300 °C, FEA modelling showed a steady state BFS temperature of 30.12 °C In a single layer array configuration, the insulated structure presented a compressive strength and energy absorption of 119.41 MPa and 2588.41 kJ m⁻³, respectively The elimination of cavity radiation greatly improved the thermal performance of the structures The lattice configuration of the sandwich structure had the highest degree of insulative performance, resulting in a BFS temperature of 701.03 °C with a heating rate of 3.1 °C/s under a thermal load of 1000 °C 	[100]
2015	Actively cooled kagome	C _f /C	Aviation kerosene	<img alt="Two diagrams of a kagome lattice structure. The top diagram shows a cross-section with labels Y=15, Y=0, X=0, X=1, X=2, X=3, X=4, X=5, X=6, X=7, X=8, X=9, X=10, X=11, X=12, X=13, X=14, X=15, X=16, X=17, X=18, X=19, X=20, X=21, X=22, X=23, X=24, X=25, X=26, X=27, X=28, X=29, X=30, X=31, X=32, X=33, X=34, X=35, X=36, X=37, X=38, X=39, X=40, X=41, X=42, X=43, X=44, X=45, X=46, X=47, X=48, X=49, X=50, X=51, X=52, X=53, X=54, X=55, X=56, X=57, X=58, X=59, X=60, X=61, X=62, X=63, X=64, X=65, X=66, X=67, X=68, X=69, X=70, X=71, X=72, X=73, X=74, X=75, X=76, X=77, X=78, X=79, X=80, X=81, X=82, X=83, X=84, X=85, X=86, X=87, X=88, X=89, X=90, X=91, X=92, X=93, X=94, X=95, X=96, X=97, X=98, X=99, X=100, X=101, X=102, X=103, X=104, X=105, X=106, X=107, X=108, X=109, X=110, X=111, X=112, X=113, X=114, X=115, X=116, X=117, X=118, X=119, X=120, X=121, X=122, X=123, X=124, X=125, X=126, X=127, X=128, X=129, X=130, X=131, X=132, X=133, X=134, X=135, X=136, X=137, X=138, X=139, X=140, X=141, X=142, X=143, X=144, X=145, X=146, X=147, X=148, X=149, X=150, X=151, X=152, X=153, X=154, X=155, X=156, X=157, X=158, X=159, X=160, X=161, X=162, X=163, X=164, X=165, X=166, X=167, X=168, X=169, X=170, X=171, X=172, X=173, X=174, X=175, X=176, X=177, X=178, X=179, X=180, X=181, X=182, X=183, X=184, X=185, X=186, X=187, X=188, X=189, X=190, X=191, X=192, X=193, X=194, X=195, X=196, X=197, X=198, X=199, X=200, X=201, X=202, X=203, X=204, X=205, X=206, X=207, X=208, X=209, X=210, X=211, X=212, X=213, X=214, X=215, X=216, X=217, X=218, X=219, X=220, X=221, X=222, X=223, X=224, X=225, X=226, X=227, X=228, X=229, X=230, X=231, X=232, X=233, X=234, X=235, X=236, X=237, X=238, X=239, X=240, X=241, X=242, X=243, X=244, X=245, X=246, X=247, X=248, X=249, X=250, X=251, X=252, X=253, X=254, X=255, X=256, X=257, X=258, X=259, X=260, X=261, X=262, X=263, X=264, X=265, X=266, X=267, X=268, X=269, X=270, X=271, X=272, X=273, X=274, X=275, X=276, X=277, X=278, X=279, X=280, X=281, X=282, X=283, X=284, X=285, X=286, X=287, X=288, X=289, X=290, X=291, X=292, X=293, X=294, X=295, X=296, X=297, X=298, X=299, X=300, X=301, X=302, X=303, X=304, X=305, X=306, X=307, X=308, X=309, X=310, X=311, X=312, X=313, X=314, X=315, X=316, X=317, X=318, X=319, X=320, X=321, X=322, X=323, X=324, X=325, X=326, X=327, X=328, X=329, X=330, X=331, X=332, X=333, X=334, X=335, X=336, X=337, X=338, X=339, X=340, X=341, X=342, X=343, X=344, X=345, X=346, X=347, X=348, X=349, X=350, X=351, X=352, X=353, X=354, X=355, X=356, X=357, X=358, X=359, X=360, X=361, X=362, X=363, X=364, X=365, X=366, X=367, X=368, X=369, X=370, X=371, X=372, X=373, X=374, X=375, X=376, X=377, X=378, X=379, X=380, X=381, X=382, X=383, X=384, X=385, X=386, X=387, X=388, X=389, X=390, X=391, X=392, X=393, X=394, X=395, X=396, X=397, X=398, X=399, X=400, X=401, X=402, X=403, X=404, X=405, X=406, X=407, X=408, X=409, X=410, X=411, X=412, X=413, X=414, X=415, X=416, X=417, X=418, X=419, X=420, X=421, X=422, X=423, X=424, X=425, X=426, X=427, X=428, X=429, X=430, X=431, X=432, X=433, X=434, X=435, X=436, X=437, X=438, X=439, X=440, X=441, X=442, X=443, X=444, X=445, X=446, X=447, X=448, X=449, X=450, X=451, X=452, X=453, X=454, X=455, X=456, X=457, X=458, X=459, X=460, X=461, X=462, X=463, X=464, X=465, X=466, X=467, X=468, X=469, X=470, X=471, X=472, X=473, X=474, X=475, X=476, X=477, X=478, X=479, X=480, X=481, X=482, X=483, X=484, X=485, X=486, X=487, X=488, X=489, X=490, X=491, X=492, X=493, X=494, X=495, X=496, X=497, X=498, X=499, X=500, X=501, X=502, X=503, X=504, X=505, X=506, X=507, X=508, X=509, X=510, X=511, X=512, X=513, X=514, X=515, X=516, X=517, X=518, X=519, X=520, X=521, X=522, X=523, X=524, X=525, X=526, X=527, X=528, X=529, X=530, X=531, X=532, X=533, X=534, X=535, X=536, X=537, X=538, X=539, X=540, X=541, X=542, X=543, X=544, X=545, X=546, X=547, X=548, X=549, X=550, X=551, X=552, X=553, X=554, X=555, X=556, X=557, X=558, X=559, X=560, X=561, X=562, X=563, X=564, X=565, X=566, X=567, X=568, X=569, X=560, X=561, X=562, X=563, X=564, X=565, X=566, X=567, X=568, X=569, X=570, X=571, X=572, X=573, X=574, X=575, X=576, X=577, X=578, X=579, X=580, X=581, X=582, X=583, X=584, X=585, X=586, X=587, X=588, X=589, X=580, X=581, X=582, X=583, X=584, X=585, X=586, X=587, X=588, X=589, X=590, X=591, X=592, X=593, X=594, X=595, X=596, X=597, X=598, X=599, X=590, X=591, X=592, X=593, X=594, X=595, X=596, X=597, X=598, X=599, X=600, X=601, X=602, X=603, X=604, X=605, X=606, X=607, X=608, X=609, X=600, X=601, X=602, X=603, X=604, X=605, X=606, X=607, X=608, X=609, X=610, X=611, X=612, X=613, X=614, X=615, X=616, X=617, X=618, X=619, X=610, X=611, X=612, X=613, X=614, X=615, X=616, X=617, X=618, X=619, X=620, X=621, X=622, X=623, X=624, X=625, X=626, X=627, X=628, X=629, X=620, X=621, X=622, X=623, X=624, X=625, X=626, X=627, X=628, X=629, X=630, X=631, X=632, X=633, X=634, X=635, X=636, X=637, X=638, X=639, X=630, X=631, X=632, X=633, X=634, X=635, X=636, X=637, X=638, X=639, X=640, X=641, X=642, X=643, X=644, X=645, X=646, X=647, X=648, X=649, X=640, X=641, X=642, X=643, X=644, X=645, X=646, X=647, X=648, X=649, X=650, X=651, X=652, X=653, X=654, X=655, X=656, X=657, X=658, X=659, X=650, X=651, X=652, X=653, X=654, X=655, X=656, X=657, X=658, X=659, X=660, X=661, X=662, X=663, X=664, X=665, X=666, X=667, X=668, X=669, X=660, X=661, X=662, X=663, X=664, X=665, X=666, X=667, X=668, X=669, X=670, X=671, X=672, X=673, X=674, X=675, X=676, X=677, X=678, X=679, X=670, X=671, X=672, X=673, X=674, X=675, X=676, X=677, X=678, X=679, X=680, X=681, X=682, X=683, X=684, X=685, X=686, X=687, X=688, X=689, X=680, X=681, X=682, X=683, X=684, X=685, X=686, X=687, X=688, X=689, X=690, X=691, X=692, X=693, X=694, X=695, X=696, X=697, X=698, X=699, X=690, X=691, X=692, X=693, X=694, X=695, X=696, X=697, X=698, X=699, X=700, X=701, X=702, X=703, X=704, X=705, X=706, X=707, X=708, X=709, X=700, X=701, X=702, X=703, X=704, X=705, X=706, X=707, X=708, X=709, X=710, X=711, X=712, X=713, X=714, X=715, X=716, X=717, X=718, X=719, X=710, X=711, X=712, X=713, X=714, X=715, X=716, X=717, X=718, X=719, X=720, X=721, X=722, X=723, X=724, X=725, X=726, X=727, X=728, X=729, X=720, X=721, X=722, X=723, X=724, X=725, X=726, X=727, X=728, X=729, X=730, X=731, X=732, X=733, X=734, X=735, X=736, X=737, X=738, X=739, X=730, X=731, X=732, X=733, X=734, X=735, X=736, X=737, X=738, X=739, X=740, X=741, X=742, X=743, X=744, X=745, X=746, X=747, X=748, X=749, X=740, X=741, X=742, X=743, X=744, X=745, X=746, X=747, X=748, X=749, X=750, X=751, X=752, X=753, X=754, X=755, X=756, X=757, X=758, X=759, X=750, X=751, X=752, X=753, X=754, X=755, X=756, X=757, X=758, X=759, X=760, X=761, X=762, X=763, X=764, X=765, X=766, X=767, X=768, X=769, X=760, X=761, X=762, X=763, X=764, X=765, X=766, X=767, X=768, X=769, X=770, X=771, X=772, X=773, X=774, X=775, X=776, X=777, X=778, X=779, X=770, X=771, X=772, X=773, X=774, X=775, X=776, X=777, X=778, X=779, X=780, X=781, X=782, X=783, X=784, X=785, X=786, X=787, X=788, X=789, X=780, X=781, X=782, X=783, X=784, X=785, X=786, X=787, X=788, X=789, X=790, X=791, X=792, X=793, X=794, X=795, X=796, X=797, X=798, X=799, X=790, X=791, X=792, X=793, X=794, X=795, X=796, X=797, X=798, X=799, X=800, X=801, X=802, X=803, X=804, X=805, X=806, X=807, X=808, X=809, X=800, X=801, X=802, X=803, X=804, X=805, X=806, X=807, X=808, X=809, X=810, X=811, X=812, X=813, X=814, X=815, X=816, X=817, X=818, X=819, X=810, X=811, X=812, X=813, X=814, X=815, X=816, X=817, X=818, X=819, X=820, X=821, X=822, X=823, X=824, X=825, X=826, X=827, X=828, X=829, X=820, X=821, X=822, X=823, X=824, X=825, X=826, X=827, X=828, X=829, X=830, X=831, X=832, X=833, X=834, X=835, X=836, X=837, X=838, X=839, X=830, X=831, X=832, X=833, X=834, X=835, X=836, X=837, X=838, X=839, X=840, X=841, X=842, X=843, X=844, X=845, X=846, X=847, X=848, X=849, X=840, X=841, X=842, X=843, X=844, X=845, X=846, X=847, X=848, X=849, X=850, X=851, X=852, X=853, X=854, X=855, X=856, X=857, X=858, X=859, X=850, X=851, X=852, X=853, X=854, X=855, X=856, X=857, X=858, X=859, X=860, X=861, X=862, X=863, X=864, X=865, X=866, X=867, X=868, X=869, X=860, X=861, X=862, X=863, X=864, X=865, X=866, X=867, X=868, X=869, X=870, X=871, X=872, X=873, X=874, X=875, X=876, X=877, X=878, X=879, X=870, X=871, X=872, X=873, X=874, X=875, X=876, X=877, X=878, X=879, X=880, X=881, X=882, X=883, X=884, X=885, X=886, X=887, X=888, X=889, X=880, X=881, X=882, X=883, X=884, X=885, X=886, X=887, X=888, X=889, X=890, X=891, X=892, X=893, X=894, X=895, X=896, X=897, X=898, X=899, X=890, X=891, X=892, X=893, X=894, X=895, X=896, X=897, X=898, X=899, X=900, X=901, X=902, X=903, X=904, X=905, X=906, X=907, X=908, X=909, X=900, X=901, X=902, X=903, X=904, X=905, X=906, X=907, X=908, X=909, X=910, X=911, X=912, X=913, X=914, X=915, X=916, X=917, X=918, X=919, X=910, X=911, X=912, X=913, X=914, X=915, X=916, X=917, X=918, X=919, X=920, X=921, X=922, X=923, X=924, X=925, X=926, X=927, X=928, X=929, X=920, X=921, X=922, X=923, X=924, X=925, X=926, X=927, X=928, X=929, X=930, X=931, X=932, X=933, X=934, X=935, X=936, X=937, X=938, X=939, X=930, X=931, X=932, X=933, X=934, X=935, X=936, X=937, X=938, X=939, X=940, X=941, X=942, X=943, X=944, X=945, X=946, X=947, X=948, X=949, X=940, X=941, X=942, X=943, X=944, X=945, X=946, X=947, X=948, X=949, X=950, X=951, X=952, X=953, X=954, X=955, X=956, X=957, X=958, X=959, X=950, X=951, X=952, X=953, X=954, X=955, X=956, X=957, X=958, X=959, X=960, X=961, X=962, X=963, X=964, X=965, X=966, X=967, X=968, X=969, X=960, X=961, X=962, X=963, X=964, X=965, X=966, X=967, X=968, X=969, X=970, X=971, X=972, X=973, X=974, X=975, X=976, X=977, X=978, X=979, X=970, X=971, X=972, X=973, X=974, X=975, X=976, X=977, X=978, X=979, X=980, X=981, X=982, X=983, X=984, X=985, X=986, X=987, X=988, X=989, X=980, X=981, X=982, X=983, X=984, X=985, X=986, X=987, X=988, X=989, X=990, X=991, X=992, X=993, X=994, X=995, X=996, X=997, X=998, X=999, X=990, X=991, X=992, X=993, X=994, X=995, X=996, X=997, X=998, X=999, X=1000, X=1001, X=1002, X=1003, X=1004, X=1005, X=1006, X=1007, X=1008, X=1009, X=1000, X=1001, X=1002, X=1003, X=1004, X=1005, X=1006, X=1007, X=1008, X=1009, X=1010, X=1011, X=1012, X=1013, X=1014, X=1015, X=1016, X=1017, X=1018, X=1019, X=1010, X=1011, X=1012, X=1013, X=1014, X=1015, X=1016, X=1017, X=1018, X=1019, X=1020, X=1021, X=1022, X=1023, X=1024, X=1025, X=1026, X=1027, X=1028, X=1029, X=1020, X=1021, X=1022, X=1023, X=1024, X=1025, X=1026, X=1027, X=1028, X=1029, X=1030, X=1031, X=1032, X=1033, X=1034, X=1035, X=1036, X=1037, X=1038, X=1039, X=1030, X=1031, X=1032, X=1033, X=1034, X=1035, X=1036, X=1037, X=1038, X=1039, X=1040, X=1041, X=1042, X=1043, X=1044, X=1045, X=1046, X=1047, X=1048, X=1049, X=1040, X=1041, X=1042, X=1043, X=1044, X=1045, X=1046, X=1047, X=1048, X=1049, X=1050, X=1051, X=1052, X=1053, X=1054, X=1055, X=1056, X=1057, X=1058, X=1059, X=1050, X=1051, X=1052, X=1053, X=1054, X=1055, X=1056, X=1057, X=1058, X=1059, X=1060, X=1061, X=1062, X=1063, X=1064, X=1065, X=1066, X=1067, X=1068, X=1069, X=1060, X=1061, X=1062, X=1063, X=1064, X=1065, X=1066, X=1067, X=1068, X=1069, X=1070, X=1071, X=1072, X=1073, X=1074, X=1075, X=1076, X=1077, X=1078, X=1079, X=1070, X=1071, X=1072, X=1073, X=1074, X=1075, X=1076, X=1077, X=1078, X=1079, X=1080, X=1081, X=1082, X=1083, X=1084, X=1085, X=1086, X=1087, X=1088, X=1089, X=1080, X=1081, X=1082, X=1083, X=1084, X=1085, X=1086, X=1087, X=1088, X=1089, X=1090, X=1091, X=1092, X=1093, X=1094, X=1095, X=1096, X=1097, X=1098, X=1099, X=1090, X=1091, X=1092, X=1093, X=1094, X=1095, X=1096, X=1097, X=1098, X=1099, X=1100, X=1101, X=1102, X=1103, X=1104, X=1105, X=1106, X=1107, X=1108, X=1109, X=1100, X=1101, X=1102, X=1103, X=1104, X=1105, X=1106, X=1107, X=1108, X=1109, X=1110, X=1111, X=1112, X=1113, X=1114, X=1115, X=1116, X=1117, X=1118, X=1119, X=1110, X=1111, X=1112, X=1113, X=1114, X=1115, X=1116, X=1117, X=1118, X=1119, X=1120, X=1121, X=1122, X=1123, X=1124, X=1125, X=1126, X=1127, X=1128, X=1129, X=1120, X=1121, X=1122, X=1123, X=1124, X=1125, X=1126, X=1127, X=1128, X=1129, X=1130, X=1131, X=1132, X=1133, X=1134, X=1135, X=1136, X=1137, X=1138, X=1139, X=1130, X=1131, X=1132, X=1133, X=1134, X=1135, X=1136, X=1137, X=1138, X=1139, X=1140, X=1141, X=1142, X=1143, X=1144, X=1145, X=1146, X=1147, X=1148, X=1			

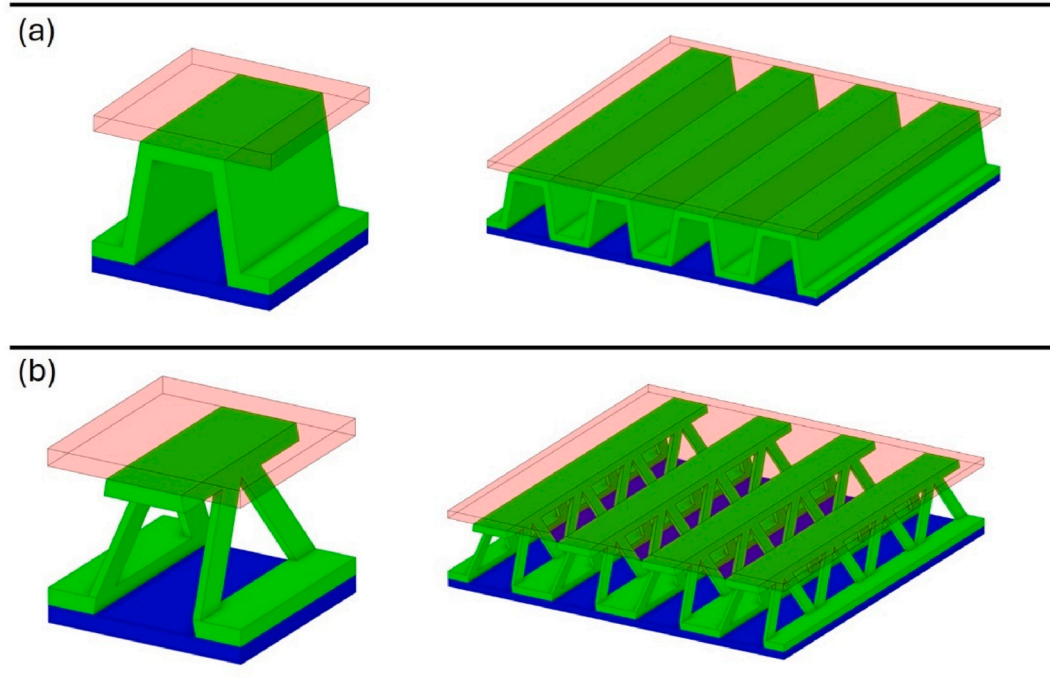


Fig. 10. Unit cell and standard sandwich configuration of (a) corrugated and (b) trapezoidal core topologies.

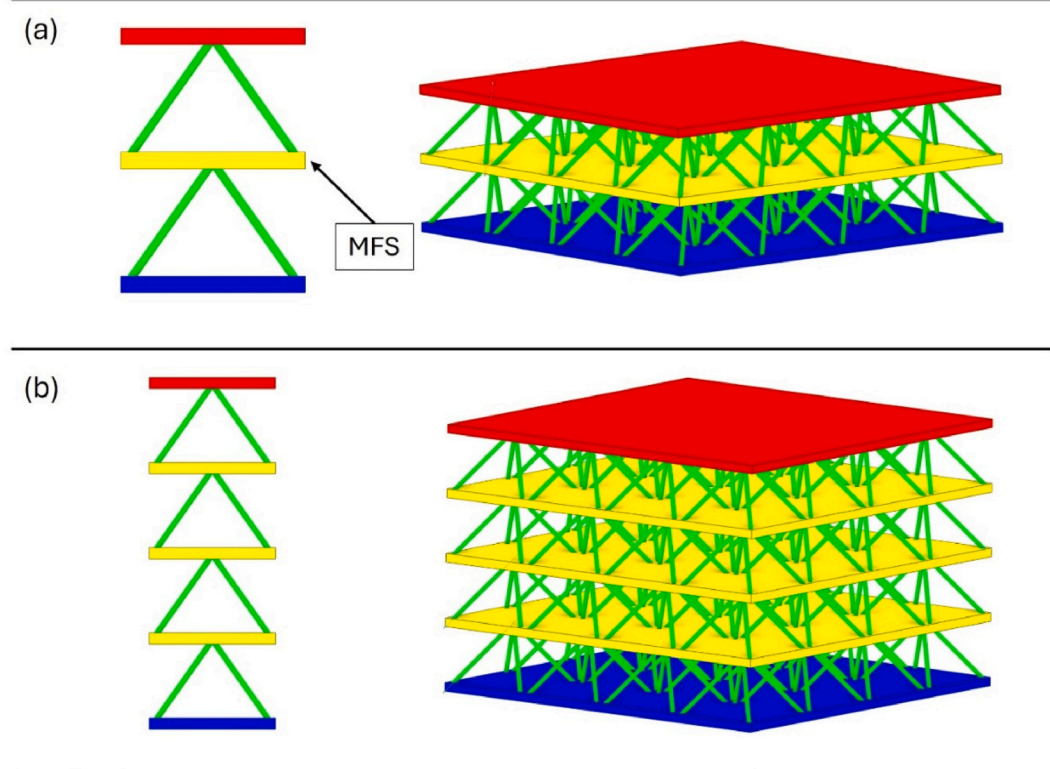


Fig. 11. Multilayered sandwich structure configuration with (a) two and (b) four layers.

configuration had a higher degree of strain tolerance than comparable honeycomb core structures, albeit with a more chaotic fracture path due to the increased presence of large imperfections. Furthermore, by following the Gibson and Ashby model of brittle fracture it was determined that the mechanical strength of logpile structures scales with relative density roughly to the power of 4–5 [104]. Further studies by

Kim et al. [103] used three and four-point bending procedures to show that the volume scaling between characteristic strength and relative density can be modelled using Weibull statistics. Overall, logpile structures were found to be stronger than honeycomb configuration when produced at the same relative density.

Tang et al. [37] investigated the high temperature insulative

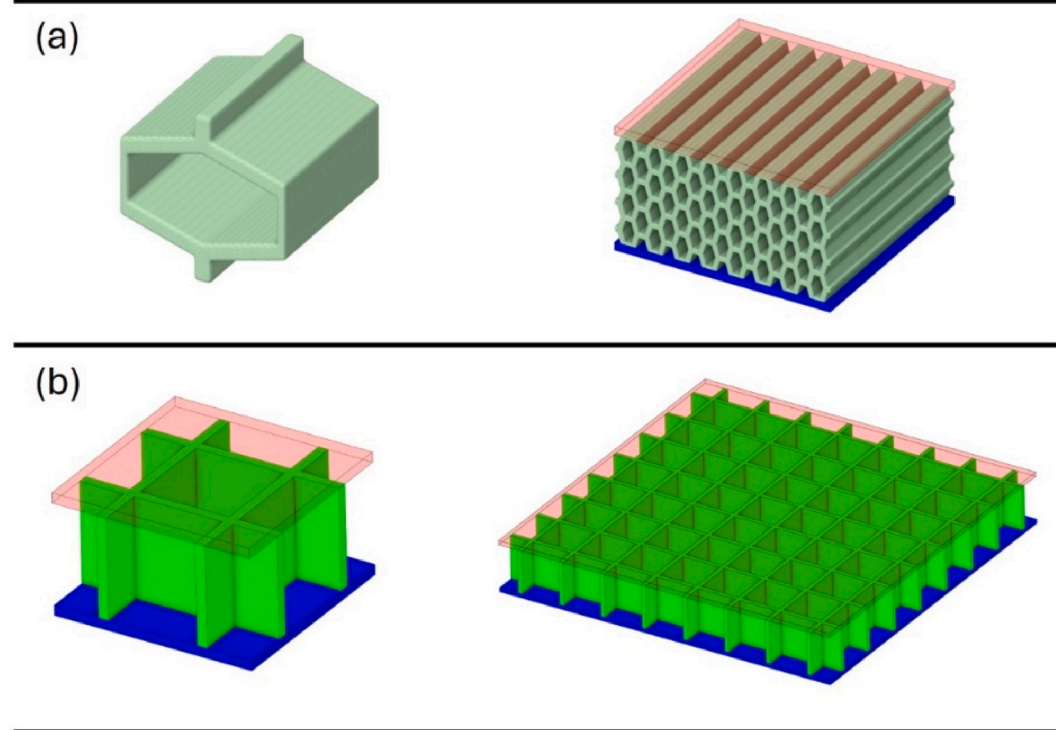


Fig. 12. Unit cell and typical sandwich structure configuration for (a) Honeycomb and (b) grid core topologies.

performance of a complex TPMS lattice core, defined by its unit cell as a gyroid architecture. The TPMS classification refers to a diverse class of periodic unit cells with zero mean curvature across each surface and continuous pores, also referred to as labyrinths, that are defined radially by the structure's porosity. The complexity of TPMS structures makes them notoriously difficult to both model and manufacture, but prior studies have reported that the unit cells possess advanced insulation characteristics and superior mechanical strength at exceptionally low relative densities [119]. Such claims are substantiated by Tang et al. [37] through thermal analysis at incremental temperature in the range of 400–1000 °C. The gyroid sandwich structures exhibit high insulative performance that is found to improve proportional to increased porosity. The heat dissipation efficiency improved with proportional increases to gyroid porosity whilst the effective thermal conductivity of the structures was reduced. The emissivity of the core was increased by approximately 0.1 over SiC, and it was observed through microstructural analysis that the surface morphology of the material plays a role in determining the final emissivity of the structure. Specifically, increasing the thickness of the microporous layer of the material is found to correlate with proportional increases to surface emissivity [37].

A subsequent study by Tang et al. [86] increased the scope of the investigation to include two additional TPMS core configurations, the Schoen I-graph and wrapped package-graph (IWP) and diamond topologies. A novel method of DLP and reactive melt infiltration was utilised to manufacture these topologies out of diamond and carbon fibre reinforced SiC. The use of diamond reinforcement was found to yield much higher mechanical performance, with significantly less strength degradation at higher temperatures compared to a C_f/SiC alternative. Of the three TPMS topologies, the diamond structure was found to present the highest mechanical strength followed by the gyroid and IWP, respectively. It was specifically noted that while the gyroid and diamond configurations include smooth internal voids which augment their mechanical strength, the struts formed within the IWP structures proved to be a prominent area of weakness leading to concentrated failure during analysis. The diamond structure formed the basis for a thermal comparison between the two materials as presented a very high insulative

capacity at temperatures between 500 and 1100 °C with effective thermal conductivities in the approximate range of 7.5 to 5.5 W (m K)⁻¹ for both diamond/SiC and C_f/SiC structures [86]. The focus on bulk material differences between the reported CMCs leads to a lack of comparative thermal performance analysis between alternative TPMS topologies.

3.3.4. Foam core

Foam structures are defined by highly porous open cell networks of randomly interconnected struts as depicted in Fig. 14. Commonly referred to as stochastic lattices, these topologies are known to be incredibly lightweight with highly insulative and energy damping characteristics [77]. A summary of key findings for experimental foam core sandwich structures is provided in Table 6.

The use of reticulated SiC foam sandwiches between C_f/SiC panels is the dominant method of foam core design for ceramic sandwich structures as the panels can be fastened to the core through the SiC matrix infiltration stage of CMC manufacture. Ortona et al. [93] describes the manufacturing of structures with and without bonded foam cores using CVI, emphasizing the improved bending strength made possible by bonding the sandwich components during manufacture. Bending strength is improved in the range of 36–67 % in structures manufactured using higher numbers of PIP cycles. Equivalent CTE properties between the core and face sheets must be maintained to maximise performance and prevent premature debonding. During three-point bend testing, the foam was seen to offer an intrinsic toughness due to the gradual fracture of individual core struts. A novel method of using electrical resistance to constantly monitor and model the integrity of the foam C_f/SiC sandwich structures is also proposed and has significant applicability to the real time operational maintenance of high-performance aerospace vehicles [121].

Hurwitz [77] describes the importance of tailoring the CTE of the core and sheet component of CMC sandwich structures to prevent internal delamination. Here, the use of Chemical Vapor Deposition (CVD) is recommended for coincident core formation and sheet siliconization. Prototype C_f/SiC sandwich structures with SiC foam cores were reported

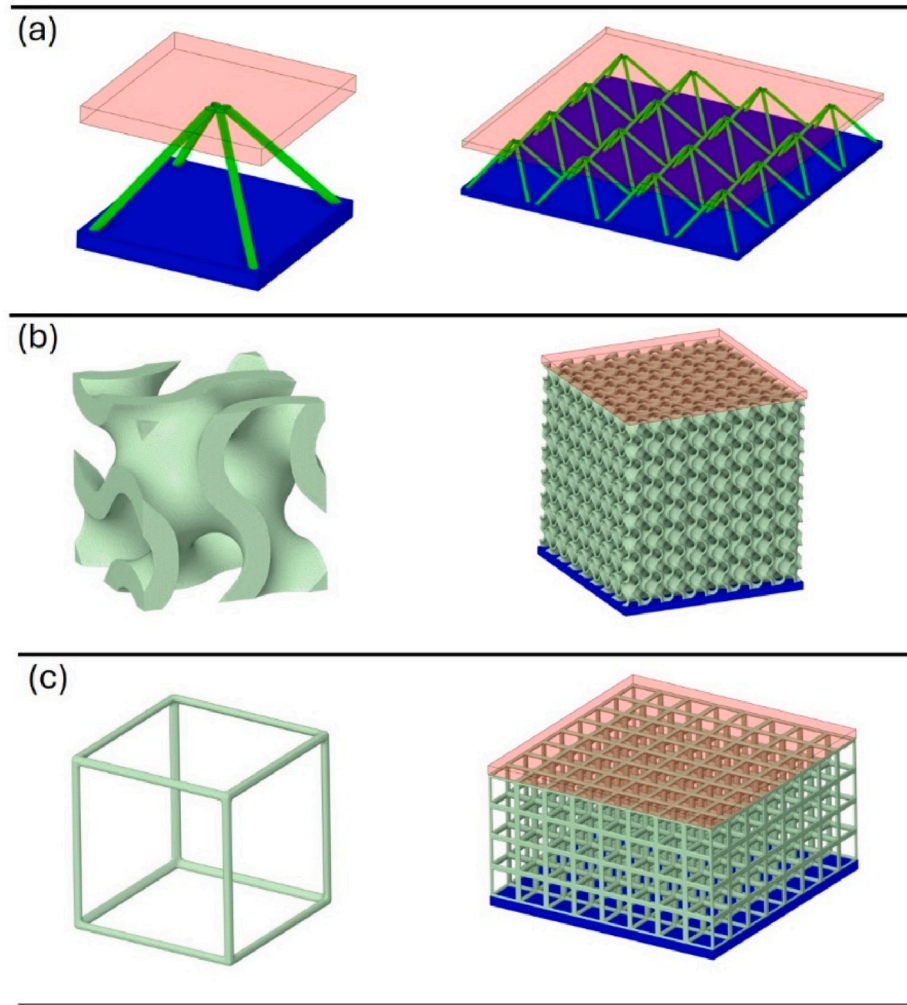


Fig. 13. Unit cells and typical sandwich structure configurations for (a) pyramidal, (b) gyroid TPMS, and (c) open cell cubic lattice core topologies.

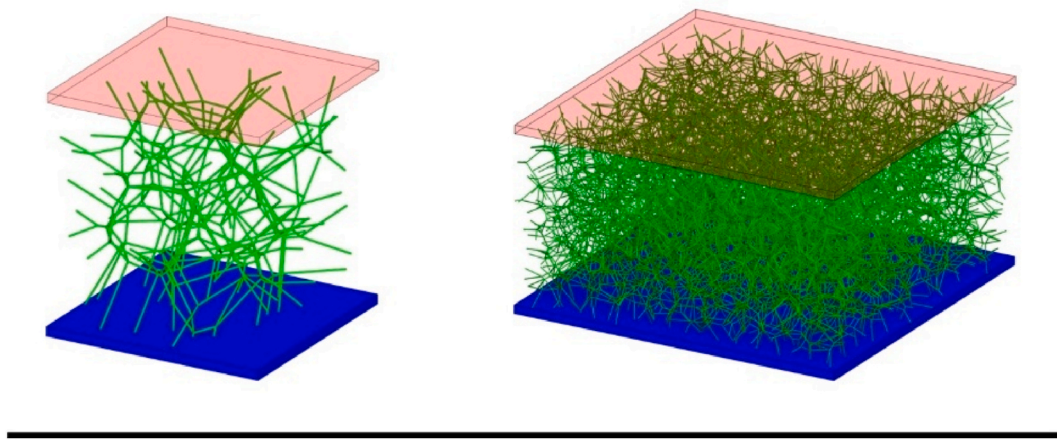


Fig. 14. Foam core sandwich structure topology.

to withstand heat flux-based load scenarios at 150 W cm^{-2} without delamination or cracking up to an internal temperature of 1000°C [77].

Gianchandani et al. [109] presented a method of joining $\text{C}_\text{f}/\text{SiC}$ and SiC/SiC face sheets to a SiC core using a composite slurry composed of Molybdenum and Silicon (MoSi_2/Si) that is placed between the sandwich components and heated to form a solid bond. Foam core sandwich

structures manufactured using this method are found to exhibit sound compressive strength properties and are able to effectively resist thermal shock at temperatures up to 1100°C [110].

Li et al. [63] investigated the influence of microstructure on the thermal shock resistance of a SiC core CMC sandwich structure using an analytical modelling approach up to 1000°C . The regularity and

periodicity of the foam was determined to be a primary factor in the resultant thermal shock strength of a foam core topology and decreases with higher cell irregularity. Foam toughness is further adversely impacted by the unstructured shape and higher number of internal cells present in its composition. Li et al. [63] concludes that the Voronoi lattice, similar to the example depicted in Fig. 14, would be more susceptible to thermal shock damage in comparison to structured sandwich core architecture.

3.4. TPS integration

The integration of additional TPS systems into ceramic sandwich structures is inferred to be in its pilot stages. The TPS breakdown of collated literature provided in Fig. 15 highlights the dominant trend of ceramic sandwich structures being developed primarily as hot structures. This correlates well with growing criticisms surrounding the complexity, weight, and cost of implementing additional methods of thermal management into the general structural design of hypersonic aircraft [4,10,122]. Regardless of the argument's validity, the prominent lack of work reported on the development of actively cooled ceramic sandwich structures is indicative of a shift in research sentiment from performance prioritisation towards economical and practically feasibility. Conversely, it marks a general underestimation into the severity of aggravated aerodynamic heating on specific components of the airframe, such as the leading edges, which are predicted to require actively cooled solutions regardless of structural performance [12]. A summary of major findings into ceramic cellular sandwich structures with TPS integration is provided in Table 7.

Exploration into the impact of internal insulation layers on the performance of the sandwich core void remains a consistent area of research. Filling the core voids with a secondary material has been shown as an effective method of reinforcing the internal sandwich supports and physically ensures thermal conduction remains the primary mechanism of heat transfer [123]. These benefits come at the cost

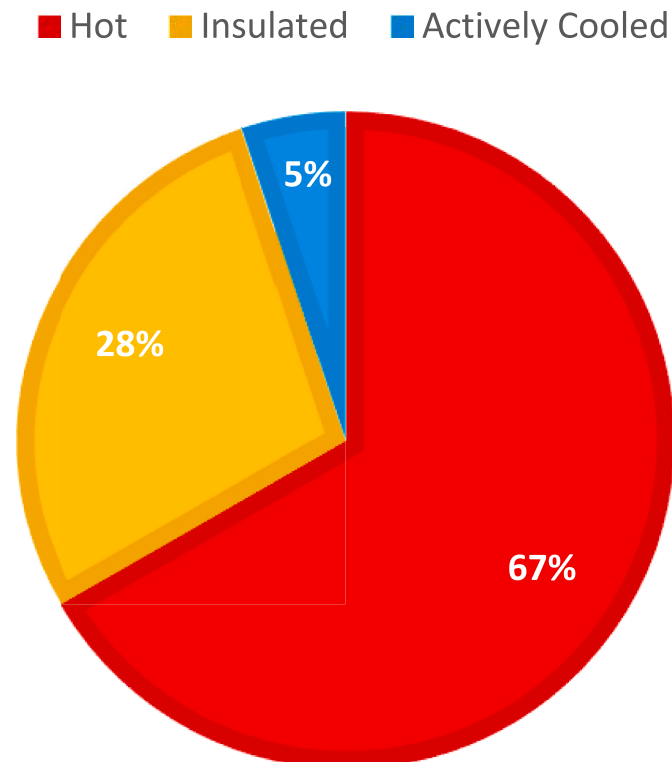


Fig. 15. Breakdown of TPS configurations integrated into hypersonic ceramic sandwich structures.

of higher relative densities and marginal increases to overall effective thermal conductivity. Moreover, feasible manufacture of these structures has proven to be a significant design challenge such that most reported studies only employ numerical analysis with little to no empirical validation.

3.4.1. Insulated ceramic sandwich structures

Current studies into insulated ceramic sandwich structures explore a range of distinct insulative materials in primary insulations configurations detailed in Fig. 16. The standard configuration depicted in Fig. 16a is the integration of a singular insulative material into the voids of the porous sandwich core. Multiple materials can be layered into the core using a method of functional grading as in Fig. 16b. This method reduces the severity of the temperature gradient acting over the sandwich structures cross-section. To enhance the thermal performance of an internally insulated structure, a layer of insulative material can be attached to the cool surface as seen in Fig. 16c [124]. The integration of phase change material layers for higher heat absorption capacity is a more experimental variation of insulation integration depicted in Fig. 16d [123].

In response to the observed steady state thermal insulation efficiency of a pyramidal $\text{C}_\text{f}/\text{SiC}$ sandwich structure being only 20 % due to cavity radiation, Wei et al. [94] integrates an unspecified aerogel into the core to enforce continuous conduction. The material was added to the investigated in a numerical heat transfer model. An approximate 700 °C reduction was recorded on the outside of the functionally insulated surface, an improvement that was attributed to the elimination of high temperature cavity radiation. The significance of this improvement showcased both the potential effectiveness of internal core insulation and quantified the severity of cavity radiation in sandwich cores of high porosity.

The influence of internal insulation on pyramidal, corrugated, and trapezoidal core $\text{C}_\text{f}/\text{SiC}$ sandwich structures was investigated by Wei et al. [125]. Numerical and analytical models are constructed to the integration of glass wool insulation under thermal and mechanical loads based on field data captured by experimental hypersonic aircraft testing [126]. The characteristic distinctions between each of the dominant core topologies are unchanged after the integration of core insulation, with pyramidal consistently demonstrating the lowest relative density comparative to the excess material requirements of corrugated configurations. This also extends to the thermal properties of each structure, as pyramidal configurations consistently provide the lowest effective thermal conductivity. Deviating from this trend, the insulated trapezoidal configurations receive the most substantial benefits to mechanical strength resulting in a structure that is both stiffer and stronger than the pyramidal or corrugated designs. Furthermore, the effectiveness of insulated ceramic sandwich structures is made more significant in consideration of their substantially lower areal density in comparison to their metallic counterparts [125].

The advantage of using insulative materials with very low thermal conductivities that are not significantly influenced by temperature is concluded by Lian et al. [127] during the numerical investigation of a trapezoidal $\text{C}_\text{f}/\text{SiC}$ sandwich structure with internal glass wool insulation. Over the course of heat transfer analysis at boundary temperature increments in the range of 1000–1600 °C it is observed that the effective thermal conductivity of a standard $\text{C}_\text{f}/\text{SiC}$ porous structure sees a 2.5x increase from 2.04 to 4.59 $\text{W m}^{-1} \text{K}^{-1}$. This is in comparison to the insulated configuration which maintains a consistent effective thermal conductivity of 0.26 $\text{W m}^{-1} \text{K}^{-1}$, although it should be noted that these conclusions are based solely on numerical approximations and would require experimental validation [127].

A $\text{C}_\text{f}/\text{SiC}$ foam core sandwich structure with a reticulated SiC core insulated by the powder deposition of a solid layer of SiO_2 was developed by Wang et al. [128]. The integration of additional solid insulation is hypothesised to provide further structural support for the highly porous stochastic SiC architecture whilst simultaneously enhancing

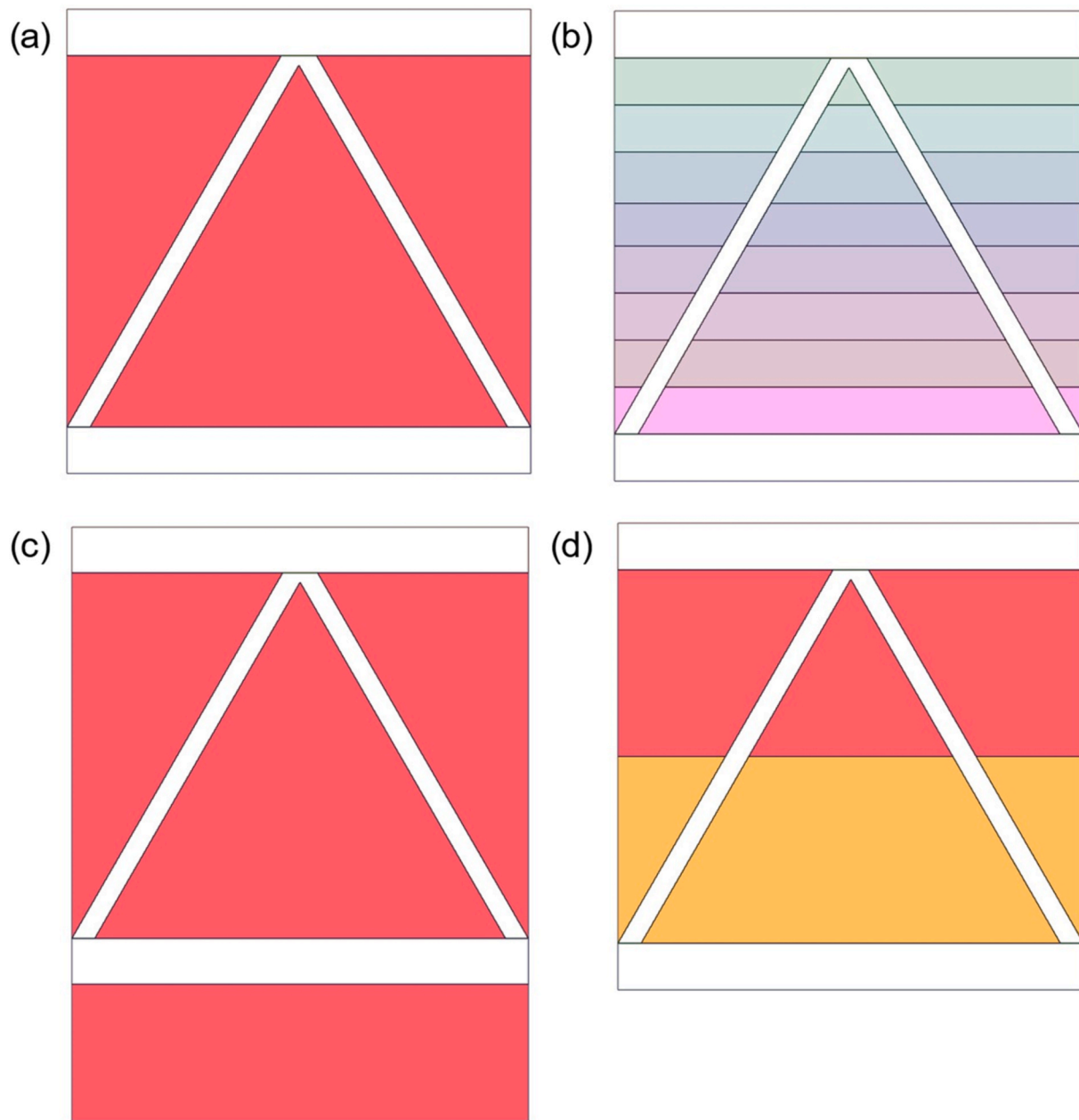


Fig. 16. Methods of sandwich structure insulation integration: (a) Uniform internal, (b) functionally graded composite layers, (c) external layer, (d) phase change layer.

insulation capacity by mitigating the effects of cavity radiation. Thermal analysis of the structure validated the hypothesised enhancements with cavity radiation successfully eliminated. As a consequence of filling the voids in the sandwich core, the governing relationship between the effective thermal conductivity and relative density subsequently becomes hypersensitive to variation of both thermal load and material density.

Ma et al. [124] outlines an analytical approach to the design of insulated corrugated core sandwich structures using only the properties and responses of the structures 2D cross-section. The methodology prioritizes maximizing the insulative efficiency of the sandwich structure by building up additional insulative materials in key regions of its cross-section. It is reported that the thermal performance of these structures can be effectively doubled by insulating the cool BFS in addition to the porous core. The additional external layers built up from the critical surface further prevent heat transfer and allow the sandwich

structure to reach safe steady state temperatures after it achieves thermal equilibrium. This approach is experimentally validated by Li et al. [68] through the design, fabrication, and simulated atmospheric re-entry wind tunnel testing of a corrugated C_f/SiC with internal and external layers of aerogel insulation. The experimental results supported a high degree of insulation performance due to the additional aerogel layers, with a BFS temperature slowly rising to a steady state of 200 °C during 1200s of heating at 1400 °C. This is a marked improvement over the 700 °C observed during the numerical analysis of the structure considering only internal insulation [68].

Chen et al. [129] transforms a trapezoidal C_f/SiC sandwich structure into a multilayered composite insulator via the integration of different insulative materials in key regions of the designs cross-section. Specifically, a thermal insulation blanket is attached to the cool BFS and a SiO₂/Al₂O₃ aerogel is inserted into the core. The optimisation of the reported ceramic TPS configuration is based on maximizing its

structural efficiency, a specialized property defining the thermo-mechanical performance of the sandwich structure as a function of relative density, core architecture and mechanical stress. The structural efficiency parameter is observed to be highly dependent on the core inclination angle, of which 30° is determined to maximise performance. The addition of both internal and external insulation greatly improves the thermal effectiveness of the sandwich structures at the cost of a consistent five-fold increase in the relative density of all core configurations.

Functional grading of multiple insulation materials in corrugated and triangular sandwich $\text{C}_\text{f}/\text{SiC}$ cores is studied by Wang et al. [130] as a method to improve overall thermal efficiency and mechanical performance. Compared to the uniform integration of a single material, graded configurations are reported to greatly lower the measured temperature of the BFS whilst maintaining high uniformity in the temperature gradient over the structures cross-section. Although, gradients formulated based on the materials bulk thermal properties are reported by Wang et al. [130] to inadequately describe transient heat transfer behaviour. Despite the potential performance advantages and promising numerical results, prototypical fabrication is made difficult given the distinct manufacturing requirements of each additional material and their careful layering within the lattice core architecture.

Mechanically, additional solid infill of the voids inside a porous lattice-core provides a significant increase to the stiffness of the structure and allow the use of more complex unit cell topologies that benefit from improved structural support. Mei et al. [100] proposes the use of Body Centred Cubic (BCC) core topologies in both array (Fig. 17a) and periodic lattice form (Fig. 17b) to construct SiC sandwich structures that are internally insulated with $\text{Q}_\text{f}/\text{SiO}_2$ aerogel layers. The SLS and sol-gel approach to sandwich structure fabrication is a found to be an effective method of streamlining the integration of internal insulation with complex core architecture. Compared to the standard single layer configuration, passive sandwich structures with bi-layered core topologies are reported to suffer from significant mechanical strength reductions that far exceed any marginal improvement to insulative performance. The compressive strength of the single layer specimens is

found to be improved by a factor of approximately 3.4 after integration of core insulation, which also reduces the rates of heating and cooling as designed. Insulated bi-layered sandwich structures provided further thermal performance enhancements at the cost of a lower mechanical strength compared to the single layer specimens.

Chen et al. [123] describes the layering of a paraffin-based Phase Change Material (PCM) to facilitate high temperature heat absorption in the core of a pyramidal $\text{C}_\text{f}/\text{SiC}$ sandwich structure. Poor PCM effectiveness is observed in a single-layer structure as the rate of heat transfer is found to outpace the phase change leading to limited heat absorption. A dual-layered configuration is proposed to create a physical barrier in the form of an MFS that is predicted to slow heat transfer and allow the phase change to take place. Further thermal resistance is integrated by the layering of solid insulation materials near the heated surface. The result is a multilayered sandwich structure configuration that presents high performance insulation under simulated boundary conditions based on empirical hypersonic flight data. A variety of PCM compositions and layered insulation configurations were proposed with the highest performance being exhibited by a paraffin/expanded graphite composition that maintained a 43.24°C BFS temperature under a heat flux-based thermal load of 2 MW m^{-2} . This configuration presented an effective thermal conductivity of only $0.82\text{ W m}^{-1}\text{ K}^{-1}$ and is recommended for further experimental study [123].

In summary, the addition of internal insulation is an attractive strategy for designers looking to improve the mechanical and thermal response of ceramic sandwich structures at the cost of a higher density and challenging fabrication process. However, the advantages of these configurations remain predominately abstract as the difficulty of prototypical manufacture has prevented comprehensive experimental analysis that would correspond with conceptual design validation.

3.4.2. Actively cooled ceramic sandwich structures

Active cooling has arisen as one of the most effective methods of integrated thermal management in hypersonic design [12]. Sandwich structures provide a desirable foundation for the integration of active cooling technology into the load bearing structural design of hypersonic

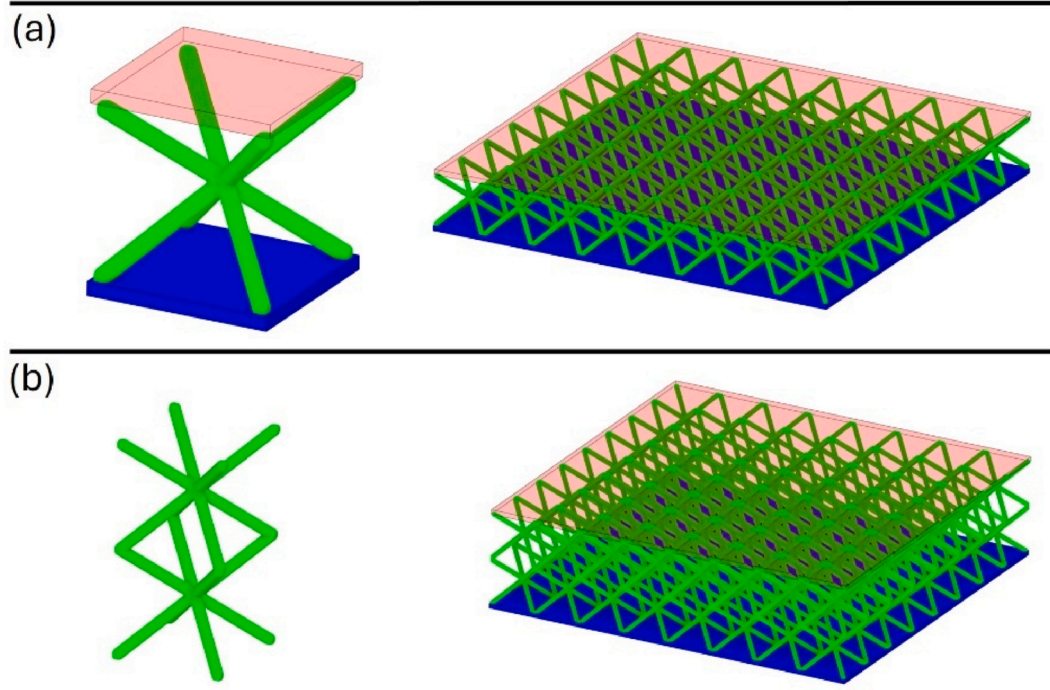


Fig. 17. Body Centred Cubic (BCC) unit cells and typical sandwich structures in (a) array and (b) periodic lattice form.

aircraft, as the core topology can be used to further enhance the forced convection heat transfer capacity of the cooling system [131]. The design of actively cooled sandwich structures therefore differs from their insulated or passive counterparts, focusing instead on balancing the weight and load bearing functionality with maximization of convective heat transfer from the core structure to the cooling fluid [69]. Research into actively cooled, solid CMC TPSSs for hypersonic aircraft has been ongoing since the turn of the century [4], however challenges associated with durability, fabrication [66], and a lack of comprehensive failure analysis [132] has dissuaded significant technological advancements in this area.

Regenerative cooling is one of the most widely studied methods of active cooling for high temperature aerospace structures, as it efficiently recirculates the vehicles fuel source as coolant before it is combusted to provide effective heat dissipation without the implementation of an independent heat sink [122]. Yu et al. [69] conducts a numerical investigation into the performance of a kerosene cooled C/C sandwich structure with a Kagome core topology (Fig. 18a) intended for use in a scramjet combustor. Compared to a passive configuration, active cooling is observed to reduce the core temperature differential by approximately 33 % and heavily mitigates the thermal stress acting throughout the core architecture. The lattice-core topology also eliminates the phenomena of coolant pyrolysis, a mechanism that has been observed to clog open cooling channels, as a result of the flow disruption caused by the Kagome unit cells [133]. However, the performance of the Kagome architecture is undermined by a distinct lack of comparison with alternative configurations. The selection of C/C, whilst prevalent in the design of rocket engine components [22,134], is not suitable for exposed regions of a hypersonic aircraft due to its incredibly poor oxidation resistance [84].

Ferrari et al. [67] designs and fabricates an actively cooled ceramic sandwich structure with a hexahedral cuboid SiSiC lattice-core topology intended to be used along a hypersonic aircrafts leading edge (Fig. 18b). This core configuration is hypothesised to enhance the forced convective heat transfer of coolant pumped through aerostructures heated aerodynamically by stagnant heating. An optimisation strategy is developed to parameterise the type of gaseous coolant and its flow rate to

determine an optimal cooling configuration. Air, Argon, and Helium are all measured at varying flow rates to simulate regenerative cooling of the leading edge. Helium is found to promote the greatest temperature reduction over the cross-section at the lowest flow rate as a result of its higher heating capacity [67]. Comparative testing of lattice-core and solid specimens are also conducted, with excellent temperature control promoted by the use of hexahedral cuboid core topology at the leading edge, indicating that the lattice-core enhances heat transfer under the airframe skin. To minimise the CTE difference between the face sheets and core, both SiC_f/SiC and $\text{C}_f/\text{C}-\text{SiC}$ panels are considered for sandwich structure design with the $\text{C}_f/\text{C}-\text{SiC}$ observed to display improved mechanical strength by comparison.

4. Conclusions, current challenges, and outlook

Whilst current research into ceramic sandwich structures for hypersonic applications maintains a consistent undercurrent of potential, with reports routinely describing a high degree of thermo-mechanical performance, persistent challenges associated with manufacturing, versatility, and efficiency continue to plague the design field. Primary challenges currently faced by researchers can be summarized by the following:

1. CMCs have become a focal point of research into ceramic sandwich structures due to their superior mechanical properties over monolithic ceramics. Unfortunately, shortcomings associated with current methods of manufacture have hindered progress towards the investigation of complex core architecture such as dense periodic lattices and TPMS structures.
2. The widespread use of CMCs in prior works has resulted in an oversaturation of studies involving simple core topologies such as pyramidal, trapezoidal, and corrugated structures. These simple structures are highly susceptible to premature failure due to high temperature cavity radiation, a phenomenon that may be mitigated topologically through the core design of dense lattice structures.
3. The integration of additional insulating materials into the sandwich core is a promising design strategy that eliminates the risk of cavity

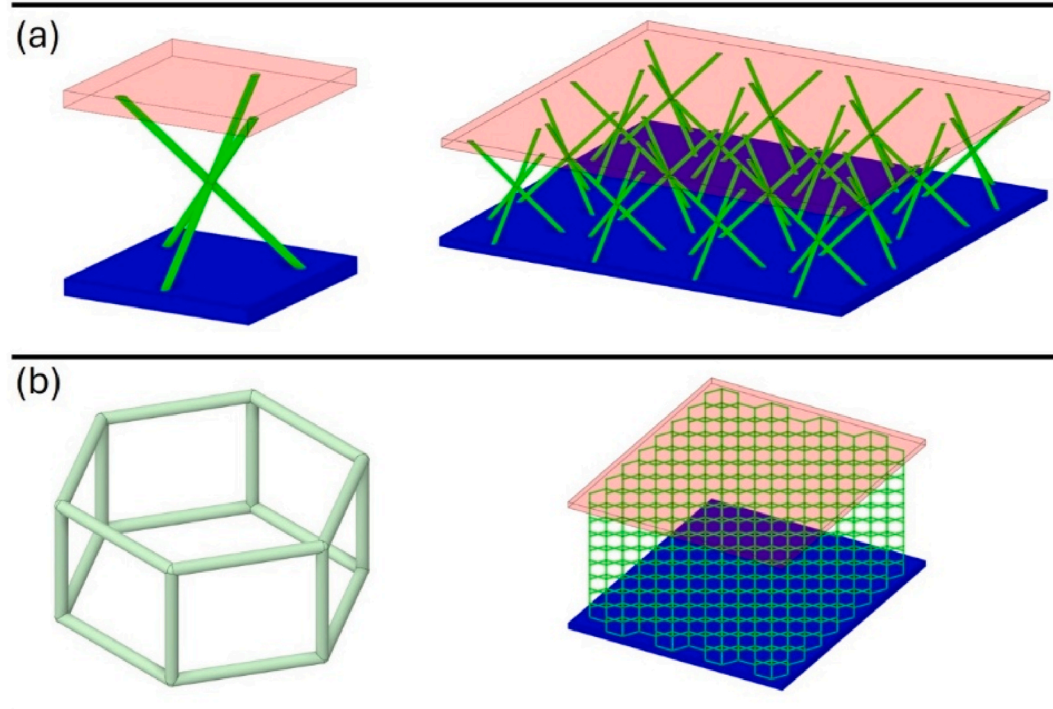


Fig. 18. Unit cell and typical sandwich structures for (a) Kagome and (b) periodic hexahedral cuboid core topologies.

radiation and reinforces the weaker core structure. Despite being a relatively active area of research, there exists a pronounced lack of prototype fabrication and experimental testing due to the intricate nature of the composites design. Current studies generally rely on numerical analysis for design validation and performance assessment, the validity of which remains uncertain until empirical validation can be undertaken. With regards to actively cooled ceramic sandwich structures, a significant amount of further research is needed based on the promising cooling performance reported by a few emerging studies.

4. Current methods of experimental and numerical analysis employed by current investigations are limited in scope, focused primarily on investigating the structures insulative efficiency through measurement of its effective thermal conductivity. Mechanically, studies rely on the use of compression and bending tests to understand a sandwich structures response to simulated aerodynamic loading or failure modes. These methods are well suited to conceptual validation of a design but ensuring reliability in the face of an extreme environment such as hypersonic aerodynamics will require more comprehensive response evaluation including, but not limited to, vibration, acoustic, impact, thermal shock, and fatigue analysis.

As the scope of research grapples with overcoming the prevalent challenges inherent to the development of CMC sandwich structures, future avenues of study should focus on diversifying the current knowledge of alternative materials and topological designs regardless of overall bulk material performance. Through building a basic understanding of the unique response elicited by different core structures of varying complexity, the optimisation potential in the design of hypersonic sandwich structures can be improved in congruence with the advancement of current manufacturing methods for high performance ceramic composites. Future studies should therefore focus on areas such as:

1. The current capabilities of ceramic AM should be incorporated to investigate the high temperature thermomechanical properties of a diverse range of highly complex core architecture, such as periodic lattices and TPMS structures, for high temperature insulative applications. This will provide foundational guidance for future designs and expand the depth of knowledge into the heat transfer characteristics of complex sandwich structures. Several studies have already been conducted in this area, but the versatility and design freedom offered by AM techniques can be expected to allow an even greater range of increasingly advanced design frameworks with specific reference to ultra-high temperature and hypersonic applications.
2. Bypassing the current limitations of CMC manufacture should be investigated using alternative ceramic materials, such as conventional technical ceramics and UHTCs. As mentioned, their compatibility with emerging AM methods will increase topological complexity in the field and expand the definition of conventional monolithic or composite ceramics in the context of high-performance aerospace applications. Improving the accessibility and capabilities of UHTC manufacture, in combination with robust AM technologies, will provide an effective method of enhancing the performance of these structures at the bulk material level.
3. Ceramic AM should also be used to apply advanced methods of structural and material-based optimisation with the goal of improving the performance and offsetting the conventional shortcomings of monolithic ceramics. For example, functional grading of the core architecture and internal material compositions have been reported to greatly improve the specific performance of ceramic structures and may prove valuable in the design of hypersonic ceramic sandwich structures [31].
4. Combining multiple materials in a single AM process should be studied as a method of integrating internal insulation into ceramic

sandwich structures. The heightened complexity of additively manufactured structures may also improve the convective heat transfer capacity of different core architecture which will increase the viability of active cooling configurations.

5. Rapid prototyping with AM should be incorporated for the investigation of more comprehensive experimental testing methodologies, alleviating the extended test specimen production times and limited part quantities.

CRediT authorship contribution statement

Jacob Bilsborough: Writing – original draft, Visualization, Validation, Methodology, Investigation, Formal analysis, Data curation, Conceptualization. **Hayley Neilsen-Burke:** Writing – review & editing, Writing – original draft. **Mehdi Khatamifar:** Writing – review & editing, Supervision. **Elsa Antunes:** Writing – review & editing, Validation, Supervision, Methodology, Conceptualization.

Declaration of competing interest

The authors declare that they have no known competing financial interests or personal relationships that could have appeared to influence the work reported in this paper.

Data availability

Data will be made available on request.

References

- [1] Bertin JJ, Cummings RM. Fifty years of hypersonics: where we've been, where we're going. *Prog Aero Sci* 2003;39:511–36. [https://doi.org/10.1016/S0376-0421\(03\)00079-4](https://doi.org/10.1016/S0376-0421(03)00079-4).
- [2] Van Wie D, D'Alessio S, White M. Hypersonic airbreathing propulsion. *Johns Hopkins APL Tech Dig* 2005;26:430–7.
- [3] Squire TH, Marschall J. Material property requirements for analysis and design of UHTC components in hypersonic applications. *J Eur Ceram Soc* 2010;30: 2239–51. <https://doi.org/10.1016/j.jeurceramsoc.2010.01.026>.
- [4] Glass D, Glass C. Airframe research and technology for hypersonic airbreathing vehicles. *AIAA/AAAF 11th int. Space planes hypersonic syst. Technol. Conf.* Orleans, France: American Institute of Aeronautics and Astronautics; 2002. <https://doi.org/10.2514/6.2002-5137>.
- [5] Musielak D. Scramjet propulsion: a practical introduction. first ed. Wiley; 2022. <https://doi.org/10.1002/9781119640646>.
- [6] Sam L, Idithsaj P, Nair PP, Suryan A, Narayanan V. Prospects for scramjet engines in reusable launch applications: a review. *Int J Hydrogen Energy* 2023; 48:36094–111. <https://doi.org/10.1016/j.ijhydene.2023.05.341>.
- [7] Fletcher DG. Fundamentals of hypersonic flow - aerothermodynamics. *Crit Technol* 2004.
- [8] Anderson JD. *Modern compressible flow: with historical perspective.* 3. ed. Boston, Mass.: McGraw-Hill; 2003.
- [9] Ohlhorst CW, Glass DE, Bruce WE, Lindell MC, Vaughn WL, Smith RW, et al. Development of X-43A mach 10 leading edges. 56th int. Astronaut. Congr. Int. Astronaut. Fed. Int. Acad. Astronaut. Int. Inst. Space law. Fukuoka, Japan: American Institute of Aeronautics and Astronautics; 2005. <https://doi.org/10.2514/6.IAC-05-D2.5.06>.
- [10] Le VT, Ha NS, Goo NS. Advanced sandwich structures for thermal protection systems in hypersonic vehicles: a review. *Compos Part B Eng* 2021;226:109301. <https://doi.org/10.1016/j.compositesb.2021.109301>.
- [11] Uyanna O, Najafi H. Thermal protection systems for space vehicles: a review on technology development, current challenges and future prospects. *Acta Astronaut* 2020;176:341–56. <https://doi.org/10.1016/j.actaastro.2020.06.047>.
- [12] Zhu Y, Peng W, Xu R, Jiang P. Review on active thermal protection and its heat transfer for airbreathing hypersonic vehicles. *Chin J Aeronaut* 2018;31:1929–53. <https://doi.org/10.1016/j.cja.2018.06.011>.
- [13] Castanie B, Bouvet C, Ginot M. Review of composite sandwich structure in aeronautic applications. *Compos Part C Open Access* 2020;1:100004. <https://doi.org/10.1016/j.jcomc.2020.100004>.
- [14] Joaniides JC, Mellin SC, Lackman LM. Mach 3 wing structures stiffened skin versus sandwich. *SAE Trans* 1961;69:167–78.
- [15] Hamer J. Honeycomb structure and its application to the concorde rudder. *Composites* 1971;2:242–5. [https://doi.org/10.1016/0010-4361\(71\)90153-4](https://doi.org/10.1016/0010-4361(71)90153-4).
- [16] Merlin PW. Mach 3 legend: design and development of the lockheed blackbird. 2012.
- [17] Sutter JK, Shin EE, Thesken JC, Fink JE. High-temperature polymer composites tested for hypersonic rocket combustor backup structure. 2005.

[18] Wu H, Koo JH. High-temperature polymers and their composites for extreme environments: a review. AIAA SCITECH 2022 forum. San Diego, CA & Virtual: American Institute of Aeronautics and Astronautics; 2022. <https://doi.org/10.2514/6.2022-1606>.

[19] Shi S, Wang Y, Yan L, Sun P, Li M, Tang S. Coupled ablation and thermal behavior of an all-composite structurally integrated thermal protection system: fabrication and modeling. *Compos Struct* 2020;251:112623. <https://doi.org/10.1016/j.compositstruct.2020.112623>.

[20] Fahrenholz W, editor. *Ultra-high temperature ceramics: materials for extreme environment applications*. Hoboken, New Jersey: ACers-Wiley; 2014.

[21] Paul A, Binner J, Vaidhyanathan B. UHTC composites for hypersonic applications. In: Fahrenholz WG, Wuchina EJ, Lee WE, Zhou Y, editors. *Ultra-high temp. Ceram.* first ed. Wiley; 2014. p. 144–66. <https://doi.org/10.1002/9781118700853.ch7>.

[22] Boyer RR, Cotton JD, Mohaghegh M, Schafrik RE. Materials considerations for aerospace applications. *MRS Bull* 2015;40:1055–66. <https://doi.org/10.1557/mrs.2015.278>.

[23] Heidenreich B. C/SiC and C/C-SiC composites. In: Bansal NP, Lamon J, editors. *Ceram. Matrix Compos.* first ed. Wiley; 2014. p. 147–216. <https://doi.org/10.1002/9781118832998.ch6>.

[24] Krenkel W, Naslain R, Schneider H, editors. *High temperature ceramic matrix composites*. Weinheim ; New York: Wiley-VCH; 2001.

[25] Dadkhah M, Tulliani J-M, Saboori A, Iuliano L. Additive manufacturing of ceramics: advances, challenges, and outlook. *J Eur Ceram Soc* 2023;43:6635–64. <https://doi.org/10.1016/j.jeurceramsoc.2023.07.033>.

[26] Sajjad U, Rehman T, Ali M, Park CW, Yan W-M. Manufacturing and potential applications of lattice structures in thermal systems: a comprehensive review of recent advances. *Int J Heat Mass Transf* 2022;198:123352. <https://doi.org/10.1016/j.ijheatmasstransfer.2022.123352>.

[27] Yang C. Preparation and thermal insulation properties of TPMS 3Y-TZP ceramics using DLP 3D printing technology. *J Mater Sci* 2023.

[28] Shen M, Qin W, Xing B, Zhao W, Gao S, Sun Y, et al. Mechanical properties of 3D printed ceramic cellular materials with triply periodic minimal surface architectures. *J Eur Ceram Soc* 2021;41:1481–9. <https://doi.org/10.1016/j.jeurceramsoc.2020.09.062>.

[29] Feng J, Fu J, Yao X, He Y. Triply periodic minimal surface (TPMS) porous structures: from multi-scale design, precise additive manufacturing to multidisciplinary applications. *Int J Extern Manuf* 2022;4:022001. <https://doi.org/10.1088/2631-7990/ac5be6>.

[30] Al-Ketan O, Lee D-W, Rowshan R, Abu Al-Rub RK. Functionally graded and multi-morphology sheet TPMS lattices: design, manufacturing, and mechanical properties. *J Mech Behav Biomed Mater* 2020;102:103520. <https://doi.org/10.1016/j.jmbbm.2019.103520>.

[31] Sestakova L, Bermejo R, Chlup Z, Danzer R. Strategies for fracture toughness, strength and reliability optimisation of ceramic-ceramic laminates. *Int J Mater Res* 2011;102:613–26. <https://doi.org/10.3139/146.110523>.

[32] Dawson DM. Ceramic materials in aerospace. In: Flower HM, editor. *High perform. Mater. Aerosp.* Dordrecht: Springer Netherlands; 1995. p. 182–201. https://doi.org/10.1007/978-94-011-0685-6_6.

[33] Birman V, Kardomateas GA. Review of current trends in research and applications of sandwich structures. *Compos Part B Eng* 2018;142:221–40. <https://doi.org/10.1016/j.compositesb.2018.01.027>.

[34] Feng Y, Qiu H, Gao Y, Zheng H, Tan J. Creative design for sandwich structures: a review. *Int J Adv Rob Syst* 2020;17:172988142092132. <https://doi.org/10.1177/1729881420921327>.

[35] Wadley HNG. Multifunctional periodic cellular metals. *Philos Trans R Soc Math Phys Eng Sci* 2006;364:31–68. <https://doi.org/10.1098/rsta.2005.1697>.

[36] Cheng X, Wei K, He R, Pei Y, Fang D. The equivalent thermal conductivity of lattice core sandwich structure: a predictive model. *Appl Therm Eng* 2016;93:236–43. <https://doi.org/10.1016/j.applthermaleng.2015.10.002>.

[37] Tang D, Xu S, Yang K, Gao T, Tang H. Effects of porosity on effective thermal conductivities of thermal insulation SiC sandwich panels with Schoen-gyroid structure. *Ceram Int* 2024;50:10618–25. <https://doi.org/10.1016/j.ceramint.2023.12.375>.

[38] Chen Y, Zhang L, Zhao Y, He R, Ai S, Tang L, et al. Mechanical behaviors of C/SiC pyramidal lattice core sandwich panel under in-plane compression. *Compos Struct* 2019;214:103–13. <https://doi.org/10.1016/j.compositstruct.2019.01.085>.

[39] Peters AB, Zhang D, Chen S, Ott C, Oses C, Curtarolo S, et al. Materials design for hypersonics. *Nat Commun* 2024;15:3328. <https://doi.org/10.1038/s41467-024-46753-3>.

[40] Dever JA, Nathal MV, DiCarlo JA. Research on high-temperature aerospace materials at NASA glenn research center. *J Aero Eng* 2013;26:500–14. [https://doi.org/10.1061/\(ASCE\)AS.1943-5525.0000321](https://doi.org/10.1061/(ASCE)AS.1943-5525.0000321).

[41] Ogasawara T, Ayabe S, Ishida Y, Aoki T, Kubota Y. Heat-resistant sandwich structure with carbon fiber-polyimide composite faces and a carbon foam core. *Compos Part Appl Sci Manuf* 2018;114:352–9. <https://doi.org/10.1016/j.compositesa.2018.08.030>.

[42] Fahrenholz WG, Hilmas GE, Talmy IG, Zaykoski JA. Refractory diborides of zirconium and hafnium. *J Am Ceram Soc* 2007;90:1347–64. <https://doi.org/10.1111/j.1551-2916.2007.01583.x>.

[43] Binner J, Porter M, Baker B, Zou J, Venkatachalam V, Diaz VR, et al. Selection, processing, properties and applications of ultra-high temperature ceramic matrix composites, UHTCMCs – a review. *Int Mater Rev* 2020;65:389–444. <https://doi.org/10.1080/09506608.2019.1652006>.

[44] Steyer TE. Shaping the future of ceramics for aerospace applications. *Int J Appl Ceram Technol* 2013;10:389–94. <https://doi.org/10.1111/ijac.12069>.

[45] Swab JJ, Jarman J, Fahrenholz W, Watts J. Mechanical properties of ZrB₂ ceramics determined by two laboratories. *Int J Appl Ceram Technol* 2023;20:3097–103. <https://doi.org/10.1111/ijac.14429>.

[46] Neuman EW, Harrington GJK, Hilmas GE, Fahrenholz WG. Thermal conductivity of hot-pressed ZrB₂-ZrC ceramics. *Materialia* 2022;26:101638. <https://doi.org/10.1016/j.mtla.2022.101638>.

[47] Savvatimskiy AI, Onufriev SV, Valyano GE, Muboyadzhyan SA. Thermophysical properties for hafnium carbide (HfC) versus temperature from 2000 to 5000 K (experiment). *J Mater Sci* 2020;55:13559–68. <https://doi.org/10.1007/s10853-020-04959-y>.

[48] Wuchina E, Opeka M, Causey S, Buesking K, Spain J, Cull A, et al. Designing for ultrahigh-temperature applications: the mechanical and thermal properties of HfB₂, HfC_x, HfNx and α Hf(N) n.d.

[49] Jin X, He R, Zhang X, Hu P. Ablation behavior of ZrB₂-SiC sharp leading edges. *J Alloys Compd* 2013;566:125–30. <https://doi.org/10.1016/j.jallcom.2013.03.067>.

[50] Fahrenholz WG. Thermodynamic analysis of ZrB₂–SiC oxidation: formation of a SiC-Depleted Region. *J Am Ceram Soc* 2007;90:143–8. <https://doi.org/10.1111/j.1551-2916.2006.01329.x>.

[51] Zhang R, He R, Zhang X, Fang D. Microstructure and mechanical properties of ZrB₂-SiC composites prepared by gelcasting and pressureless sintering. *Int J Refract Met Hard Mater* 2014;43:83–8. <https://doi.org/10.1016/j.ijrmhm.2013.11.008>.

[52] Du B, Li N, Ke B, Xing P, Jin X, Hu P, et al. ZrB₂-SiC composites' surface temperature response to dissociated oxygen at 1600 °C. *Ceram Int* 2016;42:14292–7. <https://doi.org/10.1016/j.ceramint.2016.06.041>.

[53] Johnson SM. *Thermal protection materials and systems: past and future*. Florida, USA. 2015.

[54] Johnson SM. *Ultra high temperature ceramics (UHTCs)*. 2015.

[55] Monteverde F, Bellosi A, Guicciardi S. Processing and properties of zirconium diboride-based composites. *J Eur Ceram Soc* 2002;22:279–88. [https://doi.org/10.1016/S0955-2219\(01\)00284-9](https://doi.org/10.1016/S0955-2219(01)00284-9).

[56] Cavaliere P, editor. *Spark plasma sintering of materials: advances in processing and applications*. Cham: Springer International Publishing; 2019. <https://doi.org/10.1007/978-3-030-05327-7>.

[57] Wei K, He R, Cheng X, Zhang R, Pei Y, Fang D. A lightweight, high compression strength ultra high temperature ceramic corrugated panel with potential for thermal protection system applications. *Mater Des* 2015;66:552–6. <https://doi.org/10.1016/j.matedes.2014.06.024>.

[58] Kemp JW, Diaz AA, Malek EC, Croom BP, Apostolov ZD, Kalidindi SR, et al. Direct ink writing of ZrB₂-SiC chopped fiber ceramic composites. *Addit Manuf* 2021;44:102049. <https://doi.org/10.1016/j.addma.2021.102049>.

[59] Sesso ML, Slater S, Thornton J, Franks GV. Direct ink writing of hierarchical porous ultra-high temperature ceramics (ZrB₂). *J Am Ceram Soc* 2021;104:4977–90. <https://doi.org/10.1111/jace.17911>.

[60] Peters AB, Zhang D, Nagle DC, Spicer JB. Reactive two-step additive manufacturing of ultra-high temperature carbide ceramics. *Addit Manuf* 2023;61:103318. <https://doi.org/10.1016/j.addma.2022.103318>.

[61] Peters AB, Wang C, Zhang D, Hernandez A, Nagle DC, Mueller T, et al. Reactive laser synthesis of ultra-high-temperature ceramics HfC, ZrC, TiC, HfN, ZrN, and TiN for additive manufacturing. *Ceram Int* 2023;49:11204–29. <https://doi.org/10.1016/j.ceramint.2022.11.319>.

[62] Heimbs S, Middendorf P, Kilchert S, Johnson AF, Maier M. Experimental and numerical analysis of composite folded sandwich core structures under compression. *Appl Compos Mater* 2007;14:363–77. <https://doi.org/10.1007/s10443-008-9051-9>.

[63] Li Z, Wang KF, Li JE, Wang BL, Zhang C. Effects of microstructures of foam core on the thermal shock strength of ceramic foam sandwich structures. *Materialia* 2020;10:100660. <https://doi.org/10.1016/j.mtla.2020.100660>.

[64] Liu J, Xu M, Zhang R, Zhang X, Xi W. Progress of porous/lattice structures applied in thermal management technology of aerospace applications. *Aerospace* 2022;9:827. <https://doi.org/10.3390/aerospace9120827>.

[65] Johnson SM. Approach to TPS development for hypersonic applications at NASA Ames research center. 5th eur. Workshop therm. Prot. Syst. Hot Struct., noordwijk. The Netherlands: NASA Ames Research Center; 2006.

[66] Glass D. Ceramic Matrix Composite (CMC) Thermal Protection Systems (TPS) and hot structures for hypersonic vehicles. 15th AIAA int. Space planes hypersonic syst. Technol. Conf. Dayton, Ohio: American Institute of Aeronautics and Astronautics; 2008. <https://doi.org/10.2514/6.2008-2682>.

[67] Ferrari L, Barbato M, Esser B, Petkov I, Kuhn M, Gianella S, et al. Sandwich structured ceramic matrix composites with periodic cellular ceramic cores: an active cooled thermal protection for space vehicles. *Compos Struct* 2016;154:61–8. <https://doi.org/10.1016/j.compositstruct.2016.07.043>.

[68] Li Y, Zhang L, He R, Ma Y, Zhang K, Bai X, et al. Integrated thermal protection system based on C/SiC composite corrugated core sandwich plane structure. *Aero Sci Technol* 2019;91:607–16. <https://doi.org/10.1016/j.ast.2019.05.048>.

[69] Yu J, Song QF, Ma XL, Zhao YK, Cao JH, Chen X. Study of heat transfer of composite lattice structure for active cooling used in the scramjet combustor. *Mater Res Innov* 2015;19:843–9. <https://doi.org/10.1179/1432891714Z.0000000001205>.

[70] Kausar A, Ahmad I, Rakha SA, Eisa MH, Diallo A. State-of-the-art of sandwich composite structures: manufacturing—to—high performance applications. *J Compos Sci* 2023;7:102. <https://doi.org/10.3390/jcs7030102>.

[71] Karsandik Y, Sabuncuoglu B, Yıldırım B, Silberschmidt VV. Impact behavior of sandwich composites for aviation applications: a review. *Compos Struct* 2023;314:116941. <https://doi.org/10.1016/j.compositstruct.2023.116941>.

[72] Pan B, Yu L, Wu D. Thermo-mechanical response of superalloy honeycomb sandwich panels subjected to non-steady thermal loading. *Mater Des* 2015;88: 528–36. <https://doi.org/10.1016/j.matdes.2015.09.016>.

[73] Ma Q, Rejab M, Siregar J, Guan Z. A review of the recent trends on core structures and impact response of sandwich panels. *J Compos Mater* 2021;55:2513–55. <https://doi.org/10.1177/0021998321990734>.

[74] Pan C, Han Y, Lu J. Design and optimization of lattice structures: a review. *Appl Sci* 2020;10:6374. <https://doi.org/10.3390/app10186374>.

[75] Xiong J, Du Y, Mousanezhad D, Eydani Asl M, Norato J, Vaziri A. Sandwich structures with prismatic and foam cores: a review. *Adv Eng Mater* 2019;21: 1800036. <https://doi.org/10.1002/adem.201800036>.

[76] Vijaya Ramnath B, Alagaraja K, Elanchezhan C. Review on sandwich composite and their applications. *Mater Today Proc* 2019;16:859–64. <https://doi.org/10.1016/j.matpr.2019.05.169>.

[77] Hurwitz FL. Improved fabrication of ceramic matrix composite/foam core integrated structures. *NASA Tech Briefs*; 2009;August 2009.

[78] Goodman WA, Ghasemi-Nejhad MN, Wright S, Welson D, In: Krödel M, Robichaud JL, Goodman WA, editors. T300HoneySiC: a new near-zero CTE molded C/SiC material. San Diego, California, United States; 2015. 95740E. <https://doi.org/10.1117/12.2185638>.

[79] Zhu T, Wang Z. Advances in processing and ablation properties of carbon fiber reinforced ultra-high temperature ceramic composites. *Rev Adv Mater Sci* 2024; 63:20240029. <https://doi.org/10.1515/rams-2024-0029>.

[80] Callister WD. Materials science and engineering. New York: Wiley; 2019.

[81] Röttelnbacher R, Willmann G. SiSiC — a material for high temperature ceramic heat exchangers. In: Kröckel H, Merz M, Van Der Biest O, editors. *Ceram. Adv. Energy technol.* Dordrecht: Springer Netherlands; 1984. p. 231–49. https://doi.org/10.1007/978-94-009-6424-2_13.

[82] Zhang K, Zeng T, Xu G, Cheng S, Yu S. Mechanical properties of SiCp/SiC composite lattice core sandwich panels fabricated by 3D printing combined with precursor impregnation and pyrolysis. *Compos Struct* 2020;240:112060. <https://doi.org/10.1016/j.compstruct.2020.112060>.

[83] Krenkel W. Carbon fibre reinforced silicon carbide composites (C/SiC, C/C-SiC). In: Bansal NP, editor. *Handb. Ceram. Compos.* Boston, MA: Springer US; 2005. p. 117–48. https://doi.org/10.1007/0-387-23986-3_6.

[84] Nakagawa T. 6.04 - applications of carbon/carbon composites prepared by yarn method. In: Kelly A, Zweben C, editors. *Compr. Compos. Mater.* Oxford: Pergamon; 2000. p. 47–55. <https://doi.org/10.1016/B0-08-042993-9/00210-2>.

[85] Wei K, He R, Cheng X, Zhang R, Pei Y, Fang D. Fabrication and mechanical properties of lightweight ZrO_2 ceramic corrugated core sandwich panels. *Mater Des* 2014;64:91–5. <https://doi.org/10.1016/j.matdes.2014.07.038>.

[86] Tang D, Xu S, Xu Z, He M. Ultra-temperature performance characterization of additive manufactured diamond/SiC and carbon fiber/SiC composites. *Addit Manuf* 2024;92:104381. <https://doi.org/10.1016/j.addma.2024.104381>.

[87] Liu P, Wang X, He X, Qu X. Thermal and mechanical properties of diamond/SiC substrate reinforced by bimodal diamond particles. *Carbon Lett* 2022;32:917–25. <https://doi.org/10.1007/s42823-022-00330-0>.

[88] Heidenreich B, Koch D, Kraft H, Klett Y. C/C-SiC sandwich structures manufactured via liquid silicon infiltration. *J Mater Res* 2017;32:3383–93. <https://doi.org/10.1557/jmr.2017.208>.

[89] Wei K, Peng Y, Qu Z, He R, Cheng X. High temperature mechanical behaviors of lightweight ceramic corrugated core sandwich panel. *Compos Struct* 2017;176: 379–87. <https://doi.org/10.1016/j.compstruct.2017.05.053>.

[90] Monteverde F, Bellosi A. Oxidation of ZrB_2 -Based ceramics in dry air. *J Electrochem Soc* n.d.

[91] Clougherty EV, Wilkes KE, Tye RP. Research and development of refractory oxidation-resistant diborides. Volume 5: thermal, physical, electrical and optical properties. 2. Fort Belvoir, VA: Defense Technical Information Center; 1969. <https://doi.org/10.21236/AD0865321>.

[92] Krenkel W, Berndt F. C/C-SiC composites for space applications and advanced friction systems. *Mater Sci Eng, A* 2005;412:177–81. <https://doi.org/10.1016/j.msea.2005.08.204>.

[93] Ortona A, Pusterla S, Gianella S. An integrated assembly method of sandwich structured ceramic matrix composites. *J Eur Ceram Soc* 2011;31:1821–6. <https://doi.org/10.1016/j.jeurceramsoc.2011.03.010>.

[94] Wei K, Cheng X, He R, Pei Y, Fang D. Heat transfer mechanism of the C/SiC ceramics pyramidal lattice composites. *Compos Part B Eng* 2014;63:8–14. <https://doi.org/10.1016/j.compositesb.2014.03.015>.

[95] Song Z, Cheng S, Zeng T, Yang F, Jing S, Fang D. Compressive behavior of C/SiC composite sandwich structure with stitched lattice core. *Compos Part B Eng* 2015; 69:243–8. <https://doi.org/10.1016/j.compositesb.2014.10.012>.

[96] Yang F, Cheng S, Zeng T, Wang Z, Xu G, Zhai J, et al. Mechanical and oxidation properties of C/SiC corrugated lattice core composite sandwich panels. *Compos Struct* 2016;158:137–43. <https://doi.org/10.1016/j.compstruct.2016.09.034>.

[97] Chen T, Cheng S, Jin L, Xu T, Zeng T. Fabrication process and mechanical properties of C/SiC corrugated core sandwich panel. *Ceram Int* 2021;47:3634–42. <https://doi.org/10.1016/j.ceramint.2020.09.212>.

[98] Yüzbasi NS, Graule T. Colloid casting processes: Slip casting, centrifugal casting, and gel casting. *Encycl Mater Tech Ceram Glas* 2021:146–53. <https://doi.org/10.1016/B978-0-12-803581-8.11767-9>. Elsevier.

[99] Chen A-N, Wu J-M, Liu K, Chen J-Y, Xiao H, Chen P, et al. High-performance ceramic parts with complex shape prepared by selective laser sintering: a review. *Adv Appl Ceram* 2018;117:100–17. <https://doi.org/10.1080/17436753.2017.1379586>.

[100] Mei H, Li H, Jin Z, Li L, Yang D, Liang C, et al. 3D-printed SiC lattices integrated with lightweight quartz fiber/silica aerogel sandwich structure for thermal protection system. *Chem Eng J* 2023;454:140408. <https://doi.org/10.1016/j.cej.2022.140408>.

[101] Santoliquido O, Colombo P, Ortona A. Additive manufacturing of ceramic components by Digital Light Processing: a comparison between the “bottom-up” and the “top-down” approaches. *J Eur Ceram Soc* 2019;39:2140–8. <https://doi.org/10.1016/j.jeurceramsoc.2019.01.044>.

[102] Shahzad A, Lazoglu I. Direct ink writing (DIW) of structural and functional ceramics: recent achievements and future challenges. *Compos Part B Eng* 2021; 225:109249. <https://doi.org/10.1016/j.compositesb.2021.109249>.

[103] Kim SY, Sesso ML, Franks GV. Effect of internal lattice structure on the flexural strength of 3D printed hierarchical porous ultra-high temperature ceramic (ZrB_2). *J Eur Ceram Soc* 2023;43:1762–76. <https://doi.org/10.1016/j.jeurceramsoc.2022.12.027>.

[104] Kim SY, Sesso ML, Franks GV. In-situ 4-point flexural testing and synchrotron micro X-ray computed tomography of 3D printed hierarchical-porous ultra-high temperature ceramic. *Addit Manuf* 2022;54:102728. <https://doi.org/10.1016/j.addma.2022.102728>.

[105] Kopeliovich D. Advances in the manufacture of ceramic matrix composites using infiltration techniques. *Adv Ceram Matrix Compos* 2014;79–108. <https://doi.org/10.1533/9780857098825.1.79>. Elsevier.

[106] Zhang L, Yin D, He R, Yu Z, Zhang K, Chen Y, et al. Lightweight C/SiC ceramic matrix composite structures with high loading capacity. *Adv Eng Mater* 2019;21: 1801246. <https://doi.org/10.1002/adem.201801246>.

[107] Yang F, Wang X, Zeng T, Xu G, Cheng S, Chen H. Mechanical property of C/SiC corrugated lattice core composite sandwich panels after high temperature annealing. *Compos Struct* 2019;210:687–94. <https://doi.org/10.1016/j.compstruct.2018.11.097>.

[108] Ortona A, D’Angelo C, Gianella S, Gaia D. Cellular ceramics produced by rapid prototyping and replication. *Mater Lett* 2012;80:95–8. <https://doi.org/10.1016/j.matlet.2012.04.050>.

[109] Gianchandani PK, Casalegno V, Smeacetto F, Ferraris M. Pressure-less joining of C/SiC and SiC/Si by a MoSi_2/Si composite. *Int J Appl Ceram Technol* 2017;14: 305–12. <https://doi.org/10.1111/ijac.12631>.

[110] Gianchandani PK, Casalegno V, Salvo M, Bianchi G, Ortona A, Ferraris M. SiC foam sandwich structures obtained by Mo-wrap joining. *Mater Lett* 2018;221: 240–3. <https://doi.org/10.1016/j.matlet.2018.03.105>.

[111] Bapanapalli SK. Design of an integral thermal protection system for future space vehicles. 2007.

[112] Zhang L, Chen Y, He R, Bai X, Zhang K, Ai S, et al. Bending behavior of lightweight C/SiC pyramidal lattice core sandwich panels. *Int J Mech Sci* 2020; 171:105409. <https://doi.org/10.1016/j.ijmecsci.2019.105409>.

[113] Chen Y, Zhang L, He C, He R, Xu B, Li Y. Thermal insulation performance and heat transfer mechanism of C/SiC corrugated lattice core sandwich panel. *Aero Sci Technol* 2021;111:106539. <https://doi.org/10.1016/j.ast.2021.106539>.

[114] Shi Y, Heidenreich B, Dileep PK, Koch D. Characterization and simulation of bending properties of continuous fiber reinforced C/C-SiC sandwich structures. *Key Eng Mater* 2017;742:215–22. <https://doi.org/10.4028/www.scientific.net/KEM.742.215>.

[115] Shi Y, Dileep PK, Heidenreich B, Koch D. Determination and modeling of bending properties for continuous fiber reinforced C/C-SiC sandwich structure with grid core. *Compos Struct* 2018;204:198–206. <https://doi.org/10.1016/j.compstruct.2018.07.086>.

[116] Heidenreich B, Bamsey N, Shi Y, Such-Taboada M, Koch D. Manufacture and test of C/C-SiC sandwich structures. *CEAS Space J* 2020;12:73–84. <https://doi.org/10.1007/s12567-019-00263-x>.

[117] Wang P, Fan H, Xu B, Mei J, Wu K, Wang H, et al. Collapse criteria for high temperature ceramic lattice truss materials. *Appl Therm Eng* 2015;89:505–13. <https://doi.org/10.1016/j.applthermaleng.2015.05.089>.

[118] Wei K, He R, Cheng X, Pei Y, Zhang R, Fang D. Fabrication and heat transfer characteristics of C/SiC pyramidal core lattice sandwich panel. *Appl Therm Eng* 2015;81:10–7. <https://doi.org/10.1016/j.applthermaleng.2015.02.012>.

[119] Zhou Z, Chen L, Wang W, Xing B, Tian J, Zhao Z. Effective thermal conductivity and heat transfer characteristics of a series of ceramic triply periodic minimal surface lattice structure. *Adv Eng Mater* 2023;25:2300359. <https://doi.org/10.1002/adem.202300359>.

[120] Wei K, Peng Y, Wang K, Yang F, Cheng S, Zeng T. High temperature mechanical properties of lightweight C/SiC composite pyramidal lattice core sandwich panel. *Compos Struct* 2017;178:467–75. <https://doi.org/10.1016/j.compstruct.2017.07.049>.

[121] Ortona A, D’Angelo C, Bianchi G. Monitoring sandwich structured SiC ceramics integrity by electrical resistance. *NDT E Int* 2012;46:77–82. <https://doi.org/10.1016/j.ndteint.2011.11.007>.

[122] Gou J-J, Yan Z-W, Hu J-X, Gao G, Gong C-L. The heat dissipation, transport and reuse management for hypersonic vehicles based on regenerative cooling and thermoelectric conversion. *Aero Sci Technol* 2021;108:106373. <https://doi.org/10.1016/j.ast.2020.106373>.

[123] Chen J, Hu L, Wu J, Yan Z, Chen Y, He C, et al. Bilayer lattice structure integrated with phase change material for innovative thermal protection system design. *Aero Sci Technol* 2023;141:108576. <https://doi.org/10.1016/j.ast.2023.108576>.

[124] Ma Y, Xu B, Chen M, He R, Wen W, Cheng T, et al. Optimization design of built-up thermal protection system based on validation of corrugated core homogenization. *Appl Therm Eng* 2017;115:491–500. <https://doi.org/10.1016/j.applthermaleng.2016.12.137>.

[125] Wei K, Wang X, Cheng X, Peng Y, Li M, Yang X. Structural and thermal analysis of integrated thermal protection systems with C/SiC composite cellular core

sandwich panels. *Appl Therm Eng* 2018;131:209–20. <https://doi.org/10.1016/j.applthermaleng.2017.12.009>.

[126] Meng S, Yang Q, Xie W, Han G, Du S. Structure redesign of the integrated thermal protection system and fuzzy performance evaluation. *AIAA J* 2016;54:3598–607. <https://doi.org/10.2514/1.J054996>.

[127] Lian M, Su J, He Y. Heat insulation performance of lattice thermal protection structure with reinforced plate. *J Phys Conf Ser* 2021;2044:012003. <https://doi.org/10.1088/1742-6596/2044/1/012003>.

[128] Wang Y, Chen Z, Yu S, Awuys DE, Li B, Liao J, et al. Improved sandwich structured ceramic matrix composites with excellent thermal insulation. *Compos Part B Eng* 2017;129:180–6. <https://doi.org/10.1016/j.compositesb.2017.07.068>.

[129] Chen Y, Tao Y, Xu B, Ai S, Fang D. Assessment of thermal-mechanical performance with structural efficiency concept on design of lattice-core thermal protection system. *Appl Therm Eng* 2018;143:200–8. <https://doi.org/10.1016/j.applthermaleng.2018.07.097>.

[130] Wang X, Wei K, Tao Y, Yang X, Zhou H, He R, et al. Thermal protection system integrating graded insulation materials and multilayer ceramic matrix composite cellular sandwich panels. *Compos Struct* 2019;209:523–34. <https://doi.org/10.1016/j.compstruct.2018.11.004>.

[131] Gu S, Lu TJ, Evans AG. On the design of two-dimensional cellular metals for combined heat dissipation and structural load capacity. *Int J Heat Mass Transf* 2001;44:2163–75. [https://doi.org/10.1016/S0017-9310\(00\)00234-9](https://doi.org/10.1016/S0017-9310(00)00234-9).

[132] Valdevit L, Vermaak N, Zok FW, Evans AG. A materials selection protocol for lightweight actively cooled panels. *J Appl Mech* 2008;75:061022. <https://doi.org/10.1115/1.2966270>.

[133] Al-Jothery HKM, Albarody TMB, Yusoff PSM, Abdullah MA, Hussein AR. A review of ultra-high temperature materials for thermal protection system. *IOP Conf Ser Mater Sci Eng* 2020;863:012003. <https://doi.org/10.1088/1757-899X/863/1/012003>.

[134] Langener T, Von Wolfersdorf J, Selzer M, Hald H. Experimental investigations of transpiration cooling applied to C/C material. *Int J Therm Sci* 2012;54:70–81. <https://doi.org/10.1016/j.ijthermalsci.2011.10.018>.

[135] Wei K, Cheng X, Mo F, Wen W, Fang D. Design and analysis of integrated thermal protection system based on lightweight C/SiC pyramidal lattice core sandwich panel. *Mater Des* 2016;111:435–44. <https://doi.org/10.1016/j.matdes.2016.09.021>.